




Cite this: *RSC Adv.*, 2025, 15, 25675

# Effects of hydrostatic compression and kinetic vitrification on structural relaxation behaviors of amorphous drugs: how to predict them *via* simple theoretical models?†

Tran Dinh Cuong <sup>\*,a</sup> and Anh D. Phan <sup>ab</sup>

Amorphization is considered one of the most promising strategies for enhancing pharmaceuticals' aqueous solubility and oral bioavailability. However, amorphous systems are susceptible to recrystallization because of their disordered atomic structures and elevated free energies. To resolve this problem, one needs accurate information about molecular mobilities under various physical conditions. Unfortunately, it is difficult to investigate the relaxation processes of amorphous drugs beyond the uncompressed supercooled region. Hence, we aim to develop a simple but effective toolkit to predict pharmaceuticals' relaxation time and dynamic fragility at high pressures and low temperatures. First, we apply the elastically collective nonlinear Langevin equation theory to determine the impact of local and non-local interactions on the motion of drug molecules. Then, based on the similarity between the melting transition of crystalline solids and the glass transition of soft materials, a new chemical mapping is created to connect the hydrostatic pressure, the absolute temperature, and the packing fraction. This combined approach allows us to capture the primary relaxation behaviors of amorphous drugs with minimal computational cost. Our theoretical analyses agree quantitatively well with broadband-dielectric-spectroscopy experiments in both supercooled and glassy states. Therefore, they promise to be valuable for improving the physical stability and the practical applicability of amorphous pharmaceuticals.

Received 3rd June 2025

Accepted 6th July 2025

DOI: 10.1039/d5ra03931b

rsc.li/rsc-advances

## 1. Introduction

Diseases have long been perceived as the leading threat to human well-being. According to modern studies on ancient pathogen genomics,<sup>1</sup> humanity has frequently faced the infection of *Yersinia pestis*,<sup>2</sup> *Helicobacter pylori*,<sup>3</sup> hepatitis B virus,<sup>4</sup> and parvovirus B19<sup>5</sup> since the Neolithic Age. For thousands of years, numerous catastrophic epidemics and pandemics have been recorded in human history, such as the plague of Justinian,<sup>6</sup> the Black Death,<sup>7</sup> HIV/AIDS,<sup>8</sup> Ebola,<sup>9</sup> and COVID-19.<sup>10</sup> They have not only claimed the lives of millions of people but also affected all aspects of socio-economic life severely.<sup>11–13</sup> In addition to infectious diseases, human health has been threatened by non-communicable ones, including ischaemic heart, stroke, chronic obstructive pulmonary, cancer, Alzheimer's, diabetes, and kidney.<sup>14–16</sup> As reported by the World Health Organization,<sup>17</sup> cardiovascular problems alone were

responsible for more than one-third of global deaths in 2019. Thus, it cannot be denied that disease prevention and treatment have become a deep concern for every individual, organization, and country.<sup>18–20</sup>

In the never-ending struggle against diseases, humanity has invented a crucial weapon called "drug" to deal with structural and functional disorders in living organisms.<sup>21–23</sup> Today, about 80% of marketed drugs are prepared in tablet form, and the majority exist in a crystalline state.<sup>24</sup> The most prominent advantage of pharmaceutical crystals is their superior physical and chemical stability.<sup>25,26</sup> It is feasible to maintain their quality over a prolonged period. Besides, developing synthetic and analytic methods for crystalline drugs is relatively convenient.<sup>27,28</sup> However, these pharmaceutical systems have a critical drawback: they are almost insoluble in water.<sup>29–31</sup> As an inevitable consequence, they are readily eliminated from the digestive tract before being effectively absorbed into the body.<sup>32</sup> In many cases, a large dosage of drugs is necessitated to reach therapeutic levels.<sup>33</sup> This burning issue not only occasions undesirable side effects<sup>34</sup> but also increases treatment expenses and reduces patient adherence.<sup>35</sup>

The above predicament leads to an exciting idea of changing the internal structure of pharmaceuticals from a crystalline type

<sup>a</sup>Phenikaa Institute for Advanced Study, Phenikaa University, Yen Nghia, Ha Dong, Hanoi 12116, Vietnam. E-mail: cuong.trandinh@phenikaa-uni.edu.vn

<sup>b</sup>Faculty of Materials Science and Engineering, Phenikaa University, Yen Nghia, Ha Dong, Hanoi 12116, Vietnam

† Electronic supplementary information (ESI) available. See DOI: <https://doi.org/10.1039/d5ra03931b>



with long-range order to an amorphous type with short-range order.<sup>36</sup> Fundamentally, amorphous drugs are created by cooling liquids rapidly below their melting points to inhibit nucleation processes.<sup>37</sup> Alternative techniques include hot-melt extrusion,<sup>38</sup> 3D printing,<sup>39</sup> crystal dehydration,<sup>40</sup> and solvent evaporation.<sup>41</sup> It is worth noting that the aqueous solubility of drugs is expected to increase 1.4- to 1668-fold after amorphization.<sup>42–45</sup> Accordingly, their oral bioavailability can be markedly improved.<sup>46</sup> These enormous benefits promise to open a more fruitful avenue for safeguarding human health. Yet, in practice, the applications of amorphous drugs to disease prevention and treatment remain limited due to their thermodynamic instability. Few amorphous pharmaceutical products are commercialized because recrystallization can readily occur at any stage of drug processing, such as preparation, production, and administration.<sup>47–50</sup> It is impracticable to overcome these grand challenges without intimate knowledge of molecular dynamics under different pressure–temperature ( $P$ – $T$ ) conditions.<sup>51</sup>

For the reasons above, countless attempts have been made to advance our understanding of relaxation mechanisms in amorphous drugs, particularly  $\alpha$  relaxation. On the experimental side, there has been a continuous improvement in the broadband-dielectric-spectroscopy (BDS) technique.<sup>52</sup> In the supercooled domain, the  $\alpha$  rearrangement of molecules is directly detected *via* the emergence of high, broad, and asymmetric peaks on dielectric loss spectra.<sup>53–57</sup> This approach helps experimentalists measure the structural relaxation time  $\tau_\alpha$ , the glass transition temperature  $T_g$ , and the dynamic fragility  $m$  up to hundreds of megapascals.<sup>36</sup> In the glassy domain, since molecular motions are almost frozen, the location of  $\alpha$  peaks is indirectly determined by the so-called master plot construction (MPC).<sup>58–62</sup> The MPC is considered the most reliable method for predicting the primary relaxation behaviors of amorphous pharmaceuticals at  $T < T_g$ .<sup>36</sup> However, the MPC will be invalidated if the shape of BDS spectra varies with temperature due to the contribution of excess wing and dc-conductivity.<sup>36</sup> Another way to investigate glassy dynamics is to apply the extended Adam-Gibbs model (EAGM)<sup>63–65</sup> for the entropy–mobility relationship. The EAGM allows estimating the value of  $\tau_\alpha(T < T_g)$  *via* experimental data for the structural relaxation time at  $T > T_g$  and the isobaric heat capacity at  $T = T_g$ .<sup>66</sup> Nevertheless, accurate information about the isobaric heat capacity of many pharmaceutical systems remains unavailable.<sup>51</sup> Besides, it should be noted that the EAGM only works well in the case of freshly generated non-equilibrium samples.<sup>67</sup> Consequently, how to evaluate the impact of kinetic vitrification on the structural relaxation of amorphous drugs is still a knotty question for the soft-matter community.

On the computational side, molecular dynamics (MD) simulations have been continuously enhanced to serve drug discovery and development.<sup>68</sup> MD studies can yield valuable insights into the microscopic structures, molecular interactions, stabilization mechanisms, and macroscopic properties of single- and multi-component amorphous pharmaceuticals. For instance, one can utilize MD calculations to elucidate how hydrogen-bond networks are established between drugs and

polymers, thereby finding innovative ways to design amorphous solid dispersions with high water solubilities and low recrystallization tendencies.<sup>69–71</sup> Additionally, it is viable to employ MD outputs to build solid-state descriptors and reinforce machine-learning models in pharmaceutical fields.<sup>72</sup> Despite the mentioned positive aspects, MD computations have a severe limitation: they cannot predict  $\tau_\alpha$  in a timescale larger than  $10^{-5}$  s.<sup>73–78</sup> This complicated problem principally stems from the selection of simulated temperature and annealing time.<sup>79</sup> Recall that the conventional BDS definition of the glass transition point is  $\tau_\alpha(T_g) = 10^2$  s.<sup>51</sup> Currently, there is no reliable method to extrapolate computational results for  $\tau_\alpha$  from the MD regime to the BDS one.<sup>80</sup> According to Moore's law, it would take until 2048 for the MD-BDS gap to be closed.<sup>79</sup> Hence, scientists are still looking forward to the appearance of more powerful computational tools to overcome the MD limit.

One of the most promising strategies for going beyond the MD region is to develop the elastically collective nonlinear Langevin equation (ECNLE) theory.<sup>81–83</sup> The ECNLE core idea is to view each amorphous material as a hard-sphere glass former.<sup>84</sup> In this reference system, local and non-local excitations can be effortlessly analyzed at various packing fractions  $\phi$ .<sup>85</sup> Then, based on available experimental data for bulk quantities (*e.g.*, the dimensionless isothermal compressibility or the glass transition temperature), a chemical mapping is formulated to convert ECNLE results from  $\phi$  to  $P$ – $T$  spaces.<sup>86,87</sup> This theoretical scheme enables scientists to clarify the physical properties of thermal liquids,<sup>88</sup> vdW polymers,<sup>89</sup> graphene melts,<sup>90</sup> metallic glasses,<sup>91</sup> superionic crystals,<sup>92</sup> and active pharmaceutical ingredients<sup>93</sup> in both MD and BDS timescales without heavy computational processes. Yet, current ECNLE analyses<sup>81–93</sup> cannot explain why the temperature dependence of  $\tau_\alpha$  switches from non-Arrhenius to Arrhenius-like types near kinetic vitrification.<sup>58–62</sup> The consequence is that  $\tau_\alpha$  is greatly overestimated in the glassy state.<sup>94</sup> In addition, there is a considerable discrepancy between experimental and theoretical results for  $m$  at elevated pressures.<sup>95</sup> While BDS measurements suggest that most amorphous drugs become stronger during hydrostatic compression, ECNLE calculations predict the opposite. It should be emphasized that the relaxation time, the dynamic fragility, and the recrystallization ability are closely correlated.<sup>96–98</sup> Therefore, expanding the ECNLE theory to low-temperature and high-pressure areas remains an appealing problem for research groups in the soft-matter field.

Our ultimate goal in this study is to improve the ECNLE model to capture molecular dynamics in compressed and vitrified amorphous pharmaceuticals with the tiniest computational effort. Overall, it is possible to remove ECNLE restrictions step-by-step by modifying the reference system (microscopic approach)<sup>99</sup> or the chemical mapping (macroscopic approach).<sup>92</sup> Whereas the microscopic approach can provide novel information about free-energy landscapes,<sup>91</sup> the macroscopic approach is time-saving, cost-effective, and user-friendly.<sup>100</sup> Thus, to facilitate ECNLE applications in practice, we mainly focus on the intimate relation among bulk quantities in the chemical mapping. The reference system is supposed to be unaffected by pressurization and vitrification. The



effectiveness of our ECNLE calculations is demonstrated by comparing them with cutting-edge BDS experiments.

## 2. Structural relaxation of reference system

Let us start with the ECNLE reference system constructed from an infinite number of rigid spheres with the diameter  $\sigma$  and the density  $\rho = 6\phi\pi^{-1}\sigma^{-3}$  (each sphere is equivalent to an actual molecule). Their spatial arrangement can be rapidly described by applying the well-known Percus–Yevick approximation<sup>101–103</sup> to the direct correlation function  $C(r)$ , the static structure factor  $S(k)$ , and the radial distribution function  $g(r)$ , where  $r$  is the distance and  $k$  is the wavevector. Details about  $C(r)$ ,  $S(k)$ , and  $g(r)$  can be easily found in prior ECNLE reports.<sup>90–93</sup> According to Schweizer *et al.*,<sup>104–106</sup> the motion of an arbitrary sphere (the tagged sphere) is strongly affected by its nearest-neighbor interactions, which are characterized by a non-equilibrium quantity  $F_{\text{dyn}}$  as

$$F_{\text{dyn}} = F_{\text{ideal}} + F_{\text{excess}}. \quad (1)$$

While the first term represents delocalization processes, the second term denotes confinement effects. Their mathematical expressions in real space are explicitly written by<sup>104–106</sup>

$$F_{\text{ideal}} = -3k_{\text{B}}T \ln \frac{r}{\sigma}, \quad (2)$$

$$F_{\text{excess}} = -k_{\text{B}}T \int \frac{d\vec{k}}{(2\pi)^3} \frac{\rho C^2(k)S(k)}{1 + S^{-1}(k)} e^{-\frac{1}{6}k^2r^2[1 + S^{-1}(k)]}, \quad (3)$$

where  $k_{\text{B}}$  is the Boltzmann constant.

Overall, there is competition between  $F_{\text{ideal}}$  and  $F_{\text{excess}}$  in controlling the molecular dynamics of the ECNLE reference system. At  $\phi < 0.432$ , since  $F_{\text{ideal}}$  gains the upper hand,  $F_{\text{dyn}}$  becomes a monotonically decreasing function of  $r$ .<sup>104–106</sup> That means no kinetic constraints are imposed on the tagged sphere in dilute solutions. However, the situation is reversed in dense

fluids. At  $\phi > 0.432$ ,  $F_{\text{excess}}$  prevails over  $F_{\text{ideal}}$ .<sup>104–106</sup> Accordingly, a local barrier of height  $F_{\text{B}}$  appears in the dynamic free-energy plot (Fig. 1). This event causes the tagged sphere to be temporarily trapped in an intermolecular cage of radius  $r_{\text{cage}}$ . For simplicity, we approximate  $r_{\text{cage}} \approx 1.5\sigma$  instead of solving the minimum condition of  $g(r)$ . The modulus of  $F_{\text{B}}$  is deduced from<sup>104–106</sup>

$$F_{\text{B}} = F_{\text{dyn}}(r_{\text{B}}) - F_{\text{dyn}}(r_{\text{L}}), \quad (4)$$

where  $r_{\text{B}}$  typifies the barrier position, and  $r_{\text{L}}$  symbolizes the localization length.

Interestingly, the tagged sphere tries to escape confinement by making a thermal jump of amplitude  $\Delta r = r_{\text{B}} - r_{\text{L}}$ .<sup>84,85</sup> Note that  $\Delta r$  can be up to  $0.412\sigma$  at  $\phi = 0.64$ . This value is quite large on the cage scale. Hence, a long-range deformation field has to be formed in the surroundings to create space for the activated hopping process.<sup>84,85</sup> According to the Landau–Lifshitz continuum mechanics,<sup>107</sup> the displacement  $u$  of hard spheres located at  $r \geq r_{\text{cage}}$  is determined by

$$u = \Delta r_{\text{eff}} \left( \frac{r_{\text{cage}}}{r} \right)^2, \quad (5)$$

where  $\Delta r_{\text{eff}} \approx 0.09375\Delta r^2 r_{\text{cage}}^{-1}$  describes how much the first coordination shell expands.<sup>84,85</sup> Eqn (5) shows that  $u$  is considerably shorter than  $r_{\text{L}}$ . Thus, we can view each shoved sphere as an Einstein harmonic oscillator having the force constant  $K_{\text{L}} = (\partial^2 F_{\text{dyn}} / \partial r^2)_{r=r_{\text{L}}}$  and the energy change  $\Delta F_{\text{dyn}} = K_{\text{L}}u^2/2$ . This physical picture allows computing the total strain energy  $F_{\text{E}}$  stored outside the cage by<sup>84,85</sup>

$$F_{\text{E}} = \int_{r_{\text{cage}}}^{\infty} 4\pi r^2 \rho g \Delta F_{\text{dyn}} dr \approx 12\phi \Delta r_{\text{eff}}^2 \left( \frac{r_{\text{cage}}}{\sigma} \right)^3 K_{\text{L}}. \quad (6)$$

Conspicuously, the diffusion of the tagged sphere is now affected by both local and non-local interactions. Based on the

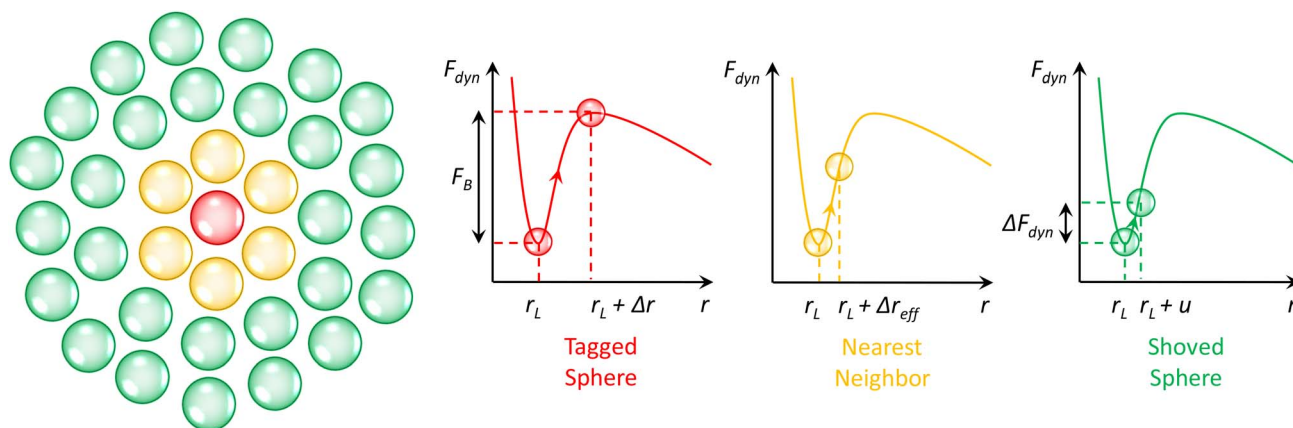


**Fig. 1** (Color online) Summarizing the prominent features of the ECNLE reference system. Whereas the distribution of hard spheres is described by the Percus–Yevick theory,<sup>101–103</sup> their interaction is modeled by the Schweizer free-energy method.<sup>104–106</sup> When the tagged sphere breaks out of the nearest neighbor cage, it distorts the first coordination shell and the remaining elastic medium.<sup>84,85</sup>



**Table 1** The local barrier  $F_B$ , the collective barrier  $F_E$ , and the structural relaxation time  $\tau_\alpha$  of the ECNLE reference system as a function of the packing fraction  $\phi$ . While  $F_B$  and  $F_E$  are in the unit of  $k_B T$ ,  $\tau_\alpha$  is in the unit of second

$\phi$	$F_B$	$F_E$	$\log_{10} \tau_\alpha$
0.440	0.0524	0.0002	−11.2298
0.445	0.1073	0.0007	−11.2131
0.450	0.1759	0.0018	−11.1905
0.455	0.2572	0.0034	−11.1651
0.460	0.3510	0.0059	−11.1377
0.465	0.4571	0.0095	−11.1090
0.470	0.5757	0.0143	−11.0789
0.475	0.7071	0.0207	−11.0475
0.480	0.8515	0.0290	−11.0149
0.485	1.0097	0.0396	−10.9808
0.490	1.1820	0.0531	−10.9450
0.495	1.3691	0.0700	−10.9071
0.500	1.5719	0.0912	−10.8665
0.505	1.7912	0.1177	−10.8223
0.510	2.0279	0.1507	−10.7733
0.515	2.2830	0.1919	−10.7179
0.520	2.5578	0.2433	−10.6532
0.525	2.8534	0.3078	−10.5755
0.530	3.1712	0.3889	−10.4796
0.535	3.5128	0.4913	−10.3586
0.540	3.8797	0.6188	−10.2043
0.545	4.2737	0.7863	−10.0076
0.550	4.6967	0.9973	−9.7610
0.555	5.1506	1.2678	−9.4579
0.560	5.6376	1.6155	−9.0932
0.565	6.1600	2.0632	−8.6602
0.570	6.7201	2.6403	−8.1497
0.575	7.3206	3.3851	−7.5473
0.580	7.9640	4.3449	−6.8333
0.585	8.6527	5.5653	−5.9875
0.590	9.3905	7.1086	−4.9817
0.595	10.1801	9.1287	−3.7496
0.600	11.0249	11.6169	−2.2904
0.605	11.9285	14.7202	−0.5395
0.610	12.8946	18.5606	1.5582
0.61095	13.0856	19.3847	2.0000
0.612	13.2995	20.3337	2.5082
0.614	13.7153	22.2559	3.5276
0.616	14.1423	24.3369	4.6210
0.618	14.5808	26.5866	5.7927
0.620	15.0311	29.0162	7.0477
0.622	15.4950	31.5123	8.3384
0.624	15.9719	34.1660	9.7036
0.626	16.4613	37.0685	11.1821
0.628	16.9628	40.3109	12.8128
0.630	17.4782	43.7995	14.5565
0.640	20.2701	65.4251	25.1874

modified Kramers theory,<sup>108–110</sup> it is feasible to infer the mean escape time or the structural relaxation time from

$$\tau_\alpha = \tau_s \left[ 1 + \frac{2\pi}{\sqrt{K_L K_B}} \frac{k_B T}{\sigma^2} \exp\left(\frac{F_B + F_E}{k_B T}\right) \right], \quad (7)$$

where  $\tau_s$  is the short relaxation timescale and  $K_B$  is the absolute curvature of the dynamic free-energy curve at  $r_B$ . Numerical results derived from eqn (4), (6), and (7) are presented in Table 1. At  $\phi < 0.55$ , because the contribution of  $F_E$  is almost negligible, the activated hopping process is mainly governed by

cage-scale dynamics. Nevertheless, an opposite trend emerges near the glass transition point ( $\phi_g \approx 0.61$ ). At  $\phi > 0.57$ , the growth rate of  $F_B$  becomes much slower than that of  $F_E$ . This event results in the dominance of collective dynamics in deeply supercooled and glassy states, consistent with experimental observations on metallic, oxide, vdW, and hydrogen-bonded materials.<sup>111</sup> Unlike MD simulations,<sup>73–79</sup> ECNLE calculations enable us to evaluate molecular mobility at various timescales spanning from picosecond to terasecond and beyond. Therefore, our theoretical data in Table 1 would be useful for designing and developing amorphous pharmaceuticals. Before applying them to a specific drug, we need to find a way to link the  $\phi$  space with its  $P$ – $T$  counterpart.<sup>86,87</sup> This work should be done quickly and accurately. So, how do we meet the above criteria? A detailed answer is revealed in subsequent sections.

### 3. Effects of hydrostatic compression

Throughout the ECNLE development journey, various strategies have been proposed to associate conceptual hard-sphere fluids with actual glass-forming liquids. Schweizer *et al.*<sup>86</sup> suggested that the  $\phi$ – $T$  relation at zero pressure would be well-quantified by combining theoretical and experimental data for the low-wavevector part of the static structure factor. This pioneering idea was proven to be effective in explaining the glassy dynamics of alkali metals, rare gases, sugar alcohols, nonpolar molecules, and vdW polymers.<sup>86,89</sup> Unfortunately, it is very challenging to apply the quasi-universal approach of Schweizer *et al.*<sup>86</sup> to amorphous pharmaceuticals due to the scarcity of equation-of-state data. To address this issue, Phan *et al.*<sup>87</sup> built another chemical mapping from the volumetric expansion of glass formers during isobaric heating. They succeeded in capturing the zero-pressure structural relaxation of unary, binary, and ternary drugs without fitting parameters.<sup>87</sup> Inspired by the works of Phan *et al.*,<sup>87</sup> Cuong *et al.*<sup>100</sup> continued to extend the ECNLE model to the high-pressure regime. The chemical mapping of Cuong *et al.*<sup>100</sup> was written by

$$\phi = \phi_0 \beta_T (T_g - T) + \phi_g, \quad (8)$$

where the initial packing fraction  $\phi_0$  was selected as 0.5 to reproduce the ECNLE outputs of Schweizer *et al.* for some typical thermal liquids.<sup>88</sup> For convenience, Cuong *et al.*<sup>100</sup> expressed the thermal expansivity  $\beta_T$  and the glass transition temperature  $T_g$  by

$$\beta_T = \frac{\beta_0}{1 + \frac{k_2}{k_3} P}, \quad (9)$$

$$T_g = k_1 \left( 1 + \frac{k_2}{k_3} P \right)^{1/k_2}. \quad (10)$$

Whereas  $\beta_0 = 12 \times 10^{-4} \text{ K}^{-1}$  was supposed to be constant for all materials,<sup>91–93</sup> the Andersson–Andersson parameters  $k_1$ ,  $k_2$ , and  $k_3$  reflected the distinctive nature of molecular bonds in the disordered state.<sup>112</sup> In contrast to  $S(k)$ , it is easy to look  $k_1$ ,  $k_2$ , and  $k_3$  up in available BDS reports on compressed amorphous





drugs.<sup>53–55</sup> Hence, Cuong *et al.*<sup>100</sup> successfully calculated the structural relaxation time of indomethacin along different isobars at breakneck speed.

In spite of the mentioned advantages, the macroscopic approach of Cuong *et al.*<sup>100</sup> still suffers from some problems. First, the physical picture behind eqn (9) is unclear. Eqn (9) is only based on the fact that the thermal expansivity and the hydrostatic pressure have a negative correlation.<sup>113</sup> We cannot naturally explain why the Andersson–Andersson parameters<sup>112</sup> appear in this formula. Second, although a good agreement between theory and experiment is achieved for  $\tau_\alpha$ , the chemical mapping of Cuong *et al.*<sup>100</sup> is not strong enough to describe the variation of  $m$  at the quantitative level. Take indomethacin as an example. At 0.1 MPa, ECNLE analyses<sup>100</sup> give  $m = 90.1$ , quite close to  $m = 82.8$  obtained from BDS measurements.<sup>114</sup> However, the higher the pressure, the larger the error. At 226 MPa, the ECNLE fragility is about 66.2,<sup>100</sup> significantly lower than the BDS counterpart of 75.2.<sup>114</sup> The underestimation of  $m$  is most likely a consequence of oversimplifying the  $\beta_T$ – $P$ – $T_g$  relation.

Herein, we remove these difficulties to gain a better description of supercooled drugs during squeezing. Our key idea is to improve eqn (9) by combining typical expansion techniques in condensed matter physics. Specifically, we begin with the following thermodynamic definition of the thermal expansivity,

$$\beta_T = \frac{1}{K_T} \left( \frac{\partial P}{\partial T} \right)_V, \quad (11)$$

where  $V$  is the molecular volume, and  $K_T$  is the isothermal bulk modulus. According to Murnaghan,<sup>115</sup> it is possible to quantify the pressure dependence of  $K_T$  *via*

$$K_T = K_0 + K'_0 P, \quad (12)$$

where  $K_0$  and  $K'_0$  are the magnitude and derivative of  $K_T$  at 0 MPa. Eqn (12) works best in a compression range  $0 \leq P \leq P_{\text{Mur}} \approx 2K_0$ .<sup>116</sup> Recent experimental evidence shows that  $P_{\text{Mur}}$  is in the order of several GPa.<sup>117–119</sup> Meanwhile, the actual production of amorphous drugs is frequently performed at  $P < 1$  GPa.<sup>51</sup> Thus, the Murnaghan approximation<sup>115</sup> is highly suitable for our study.

Next, we focus on  $(\partial P/\partial T)_V$ . In the famed Einstein picture of molecular vibrations, the contribution of thermal excitations to the hydrostatic pressure can be evaluated by<sup>120</sup>

$$\left( \frac{\partial P}{\partial T} \right)_V = \frac{3k_B \gamma_G}{V} \left( \frac{\theta_E}{T} \right)^2 \frac{e^{\theta_E/T}}{(e^{\theta_E/T} - 1)^2}. \quad (13)$$

where  $\theta_E$  is the Einstein temperature, and  $\gamma_G$  is the Gruneisen parameter. Recall that supercooled liquids primarily exist in a high-temperature region  $T_g \leq T \leq T_m$ , where  $T_m \approx 1.362T_g$  is the melting point.<sup>93</sup> Previous shock-wave experiments<sup>121</sup> and thermodynamic calculations<sup>122</sup> suggested that  $\gamma_G$  would be proportional to  $V$  under these conditions. Moreover, since the studied  $T$  value is far above  $\theta_E$ , we can replace  $e^{\theta_E/T}$  with  $1 + \theta_E/T$ . As a result, eqn (13) is simplified by

$$\left( \frac{\partial P}{\partial T} \right)_V = \text{const.} \quad (14)$$

Entering eqn (12) and (14) into eqn (11) provides

$$\beta_T = \frac{\beta_0}{1 + \frac{K'_0}{K_0} P}. \quad (15)$$

Eqn (15) highlights a close correlation between thermodynamic and mechanical quantities in the supercooled state.

Fascinatingly, we can also connect the elastic responses of materials with their glass-transition behaviors *via* ECNLE analyses in the ultra-local limit.<sup>123</sup> Utilizing the Green–Kubo formula<sup>124</sup> for the shear modulus  $G$  yields

$$G_\infty = \frac{k_B T}{60\pi^2} \int_0^\infty dk \left[ \frac{k^2}{S(k)} \frac{dS(k)}{dk} \right]^2 \exp \left[ -\frac{k^2 r_L^2}{3S(k)} \right]. \quad (16)$$

In the high-density regime, because the localization length is much shorter than the particle diameter, the main contributors to instantaneous rigidity are wavevectors with magnitudes larger than  $\pi/\sigma$ .<sup>123</sup> This insight enables us to compact eqn (16) by

$$\frac{G_g V_g}{T_g} = \frac{9}{30} k_B \left( \frac{\sigma}{r_L} \right)_{\phi=\phi_g}^2 = C_g, \quad (17)$$

where  $G_g$  and  $V_g$  are the critical values of  $G$  and  $V$  at  $T_g$ , respectively. Our numerical calculations with  $\tau_\alpha(\phi_g) = 100$  s reveal that  $C_g = 1015.6625k_B$  is a universal constant for all soft-matter systems. This finding is supported by the recent statistics of Shi *et al.*<sup>125</sup> on metallic glasses.

Eqn (17) can be seen as another definition of kinetic vitrification in the framework of the ECNLE theory. Relying on eqn (17), we can elucidate how the glass transition temperature depends on the hydrostatic pressure *via* available information about elastic moduli. Indeed, as indicated by Guinan and Steinberg,<sup>126</sup> the  $G_g$ – $P$  relation can be well described by

$$G_g(P) = G_g(0) + \left( \frac{\partial G_g}{\partial P} \right)_T \left[ \frac{V_g(P)}{V_g(0)} \right]^{1/3} P. \quad (18)$$

This simple formula is designed to reproduce the Thomas–Fermi picture of shear deformation in the  $V_g \rightarrow 0$  limit.<sup>127</sup> Since the Poisson ratio of pharmaceuticals varies slowly during compression,<sup>128</sup> eqn (18) can be rewritten by

$$G_g(P) = G_g(0) \left\{ 1 + \frac{K'_0}{K_0} \left[ \frac{V_g(P)}{V_g(0)} \right]^{1/3} P \right\}. \quad (19)$$

Besides, by integrating eqn (12), we have

$$V_g(P) = V_g(0) \left( 1 + \frac{K'_0}{K_0} P \right)^{-1/K'_0}. \quad (20)$$

Inserting eqn (19) and (20) into eqn (17) brings

$$T_g(P) = T_g(0) \left( 1 + \frac{K'_0}{K_0} P \right)^{-1/K'_0} \times \left[ 1 + \frac{K'_0}{K_0} P \left( 1 + \frac{K'_0}{K_0} P \right)^{-1/3K'_0} \right]. \quad (21)$$



Now, we can effortlessly associate volumetric dilation with kinetic vitrification. Namely, if the applied pressure is sufficiently low, eqn (21) will be equivalent to

$$T_g(P) \approx T_g(0) \left[ 1 + \frac{K'_0 - 1}{K_0} P + \frac{1}{K_0^2} \left( \frac{1}{2} - \frac{5}{6} K'_0 \right) P^2 \right]. \quad (22)$$

In addition, employing the Taylor expansion<sup>129</sup> to eqn (10) leads to

$$T_g(P) \approx k_1 \left[ 1 + \frac{1}{k_3} P + \frac{k_2}{2k_3^2} \left( \frac{1}{k_2} - 1 \right) P^2 \right]. \quad (23)$$

By equating the coefficients of eqn (22) and (23), we obtain

$$K_0 = \frac{4k_3}{\sqrt{1 + 24k_2} - 5}, \quad K'_0 = \frac{\sqrt{1 + 24k_2} - 1}{\sqrt{1 + 24k_2} - 5}. \quad (24)$$

Continuing to combine eqn (15) and (24) gives us

$$\beta_T = \frac{\beta_0}{1 + \frac{\sqrt{1 + 24k_2} - 1}{4k_3} P}. \quad (25)$$

Unlike eqn (9) and (25) possesses a solid theoretical background. That is why it can effectively characterize the degree of  $\beta_T$  reduction, as demonstrated in the case of ibuprofen<sup>130</sup> (see Fig. 2). Furthermore, applying eqn (25) to practical situations is very convenient thanks to the high availability of Andersson–Andersson parameters.<sup>53–55</sup> For the reasons above, we view it as one of the most crucial factors in deciphering the molecular dynamics of amorphous drugs *via* ECNLE calculations.

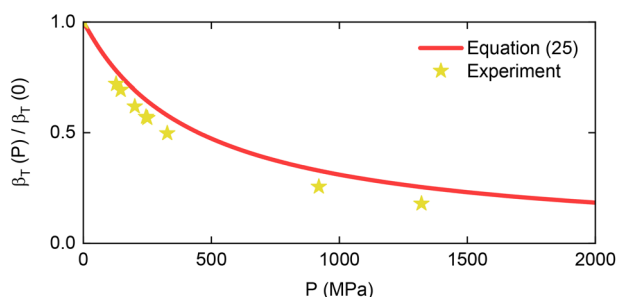


Fig. 2 (Color online) Illustrating the usefulness of eqn (25) in describing the decline of  $\beta_T$ . Ibuprofen is selected as a case study with  $k_1 = 234.7$  K,  $k_2 = 3.84$ , and  $k_3 = 970.76$  MPa. PVT measurements in ref. 130 are adopted as a benchmark for ECNLE analyses.

To further clarify the quality of our chemical mapping [eqn (8), (10), and (25)], we carry out numerical calculations for nine representative active pharmaceutical ingredients, including ketoprofen, probucol, ketoconazole, indomethacin, ticagrelor, fenofibrate, itraconazole, glibenclamide, and ibuprofen. Their Andersson–Andersson parameters are directly deduced from prior BDS measurements<sup>114,130–137</sup> and systematically presented in Table 2. More information about them can be found in Section S1 of the ESI.† It should be noted that the glass transition of soft materials is not always defined at  $\tau_\alpha = 10^2$  s. In some circumstances, experimentalists can determine  $T_g$  at a smaller timescale to avoid long extrapolations.<sup>135–138</sup> Therefore, depending on the specific BDS definition of  $T_g$ , we infer the corresponding value of  $\phi_g$  from interpolating ECNLE data in Table 1. This treatment ensures a direct comparison between theory and experiment. We also report the critical slope of the  $\log_{10} \tau_\alpha$  plot at  $\phi_g$  to facilitate the later analyses of the dynamic fragility.

Fig. 3 shows the structural relaxation time of the selected pharmaceutical systems under various thermodynamic conditions. It is conspicuous that our macroscopic approach helps regenerate most existing experimental data<sup>114,131–136,138</sup> without great computational efforts. For a given drug, we only need to spend a few minutes on our personal computer to quantitatively understand the dramatic slowing down of molecular dynamics during isobaric cooling or isothermal squeezing. In particular, no fitting procedures are required to achieve consistency between ECNLE calculations and BDS experiments from microsecond to hectosecond domains. These outstanding advantages distinguish our theory from other methods like EAGM<sup>66</sup> or MD.<sup>79</sup> Further insights into non-exponential growth in  $\tau_\alpha$  are provided in Section S2 of the ESI.†

Among the studied glass-forming liquids, only glibenclamide presents a marked discrepancy between theoretical and experimental results<sup>137</sup> in the supercooled state. From our perspective, this deviation may stem from the effects of tautomerism. It is well-known that glibenclamide samples in practice often contain two tautomeric forms called amide and imidic acid.<sup>137</sup> Each tautomer possesses unique physical characteristics, and the tautomer concentration varies with temperature, pressure, and time.<sup>139–141</sup> This complexity may result in a non-universal coupling between local and collective

Table 2 Experimental inputs to our newly developed chemical mapping. Here,  $k_1$  is in Kelvin,  $k_3$  is in megapascal, and  $\tau_\alpha$  is in second

Drug	$k_1$	$k_2$	$k_3$	$\tau_\alpha(T_g)$	$\phi_g$	$\left( \frac{\partial \log_{10} \tau_\alpha}{\partial \phi} \right)_{\phi=\phi_g}$	Reference
Ketoprofen	266.50	2.62	1344.32	100	0.61095	474.314	131
Probucol	293.80	2.08	672.32	100	0.61095	474.314	132
Ketoconazole	314.00	2.31	1366.51	100	0.61095	474.314	133
Indomethacin	315.00	3.14	1238.00	100	0.61095	474.314	114
Ticagrelor	319.00	2.31	1954.08	100	0.61095	474.314	134
Fenofibrate	253.60	2.46	1102.99	10	0.60875	436.008	135
Itraconazole	332.10	1.07	1743.06	1	0.60636	403.537	136
Glibenclamide	344.36	3.86	1382.00	1	0.60636	403.537	137
Ibuprofen	234.70	3.84	970.76	0.1	0.60377	366.294	130



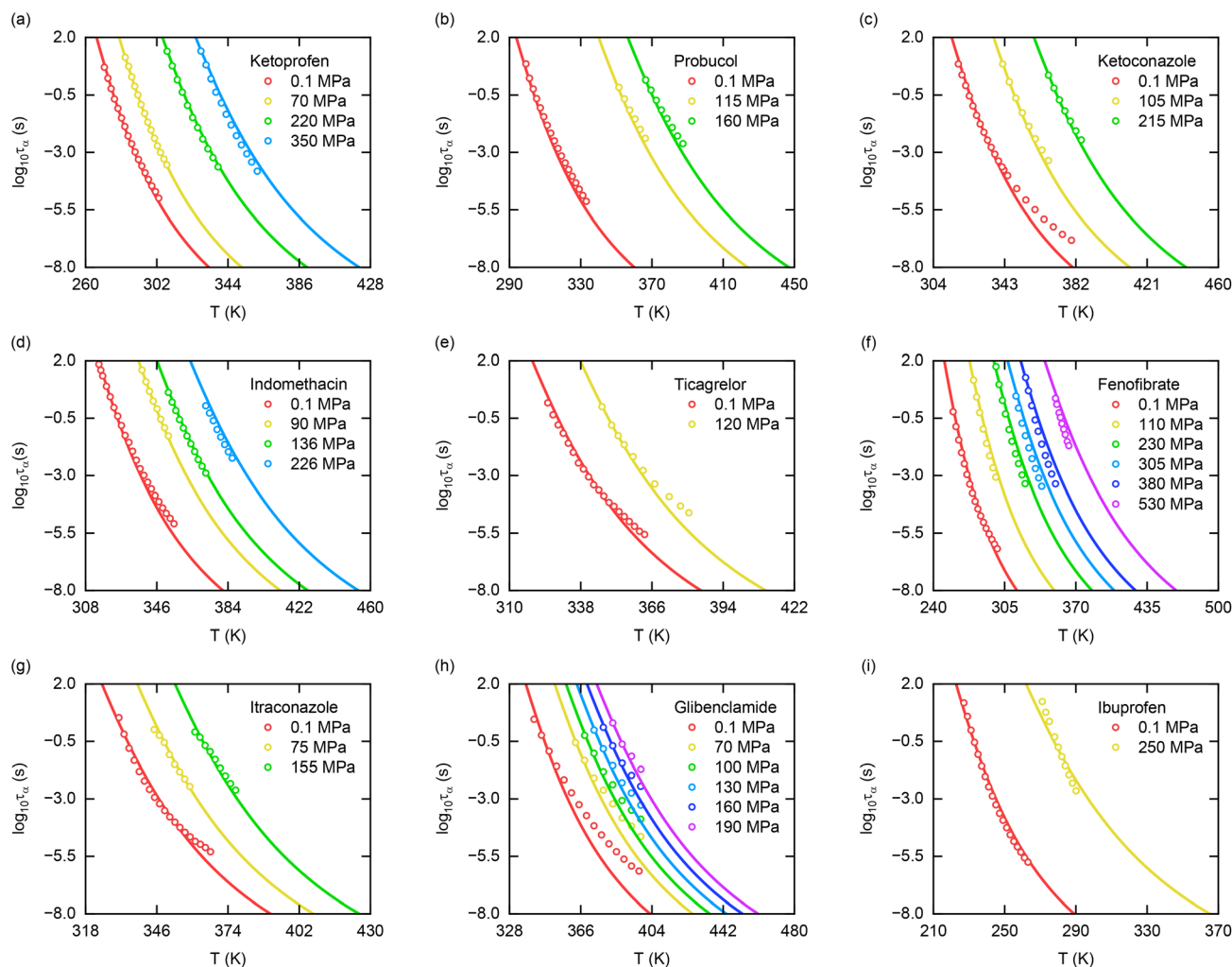


Fig. 3 (Color online) The influences of temperature and pressure on the structural relaxation time of the chosen supercooled drugs: (a) ketoprofen, (b) probutol, (c) ketoconazole, (d) indomethacin, (e) ticagrelor, (f) fenofibrate, (g) itraconazole, (h) glibenclamide, and (i) ibuprofen. While solid lines present our ECNLE calculations, open circles denote prior BDS experiments.<sup>114,131–138</sup>

dynamics in eqn (7).<sup>99</sup> Hence, the reference system and the chemical mapping should be simultaneously improved if we want to capture the structural relaxation of glibenclamide at the quantitative level.

Fig. 4 presents our ECNLE outputs for the dynamic fragility of the chosen glass formers. Fundamentally, this quantity is computed by<sup>142</sup>

$$m = \left[ \frac{\partial \log_{10} \tau_{\alpha}}{\partial (T_g/T)} \right]_{T=T_g} = \beta_T T_g \phi_0 \left( \frac{\partial \log_{10} \tau_{\alpha}}{\partial \phi} \right)_{\phi=\phi_g} \quad (26)$$

Eqn (26) confirms a strong connection between  $m$  and  $\beta_T$ , in line with recent experimental observations.<sup>143–147</sup> It also unveils why earlier theoretical studies failed to predict the pressure variation of  $m$ , even at the qualitative level. In ref. 95, researchers only focused on modeling the dynamic free energy of hard-sphere fluids and completely ignored the pressure dependence of  $\beta_T$ . Consequently, they observed a profound contradiction between theory and experiment in  $m$ - $P$  profiles,

although their estimations for  $\tau_{\alpha}$  in the high-pressure area were quite good.<sup>95</sup>

To further illuminate the underlying correlation between  $m$  and  $P$ , we rewrite eqn (26) by

$$m = k_1 \beta_0 \phi_0 \left( \frac{\partial \log_{10} \tau_{\alpha}}{\partial \phi} \right)_{\phi=\phi_g} \left( 1 + \frac{k_2}{k_3} P \right)^{\frac{1-k_2}{k_2}}, \quad (27)$$

$$m = k_1 \beta_0 \phi_0 \left( \frac{\partial \log_{10} \tau_{\alpha}}{\partial \phi} \right)_{\phi=\phi_g} \frac{\left( 1 + \frac{k_2}{k_3} P \right)^{\frac{1}{k_2}}}{1 + \frac{\sqrt{1+24k_2-1}}{4k_3} P}. \quad (28)$$

Whereas eqn (27) originates from the chemical mapping of Cuong *et al.*,<sup>100</sup> eqn (28) stems from our macroscopic approach. Both show a continuous decrease in  $m$  with increasing  $P$ . This tendency is true for the vast majority of amorphous drugs<sup>114,131–136,138</sup> except for glibenclamide,<sup>137</sup> where compression forces may significantly change the tautomeric equilibrium



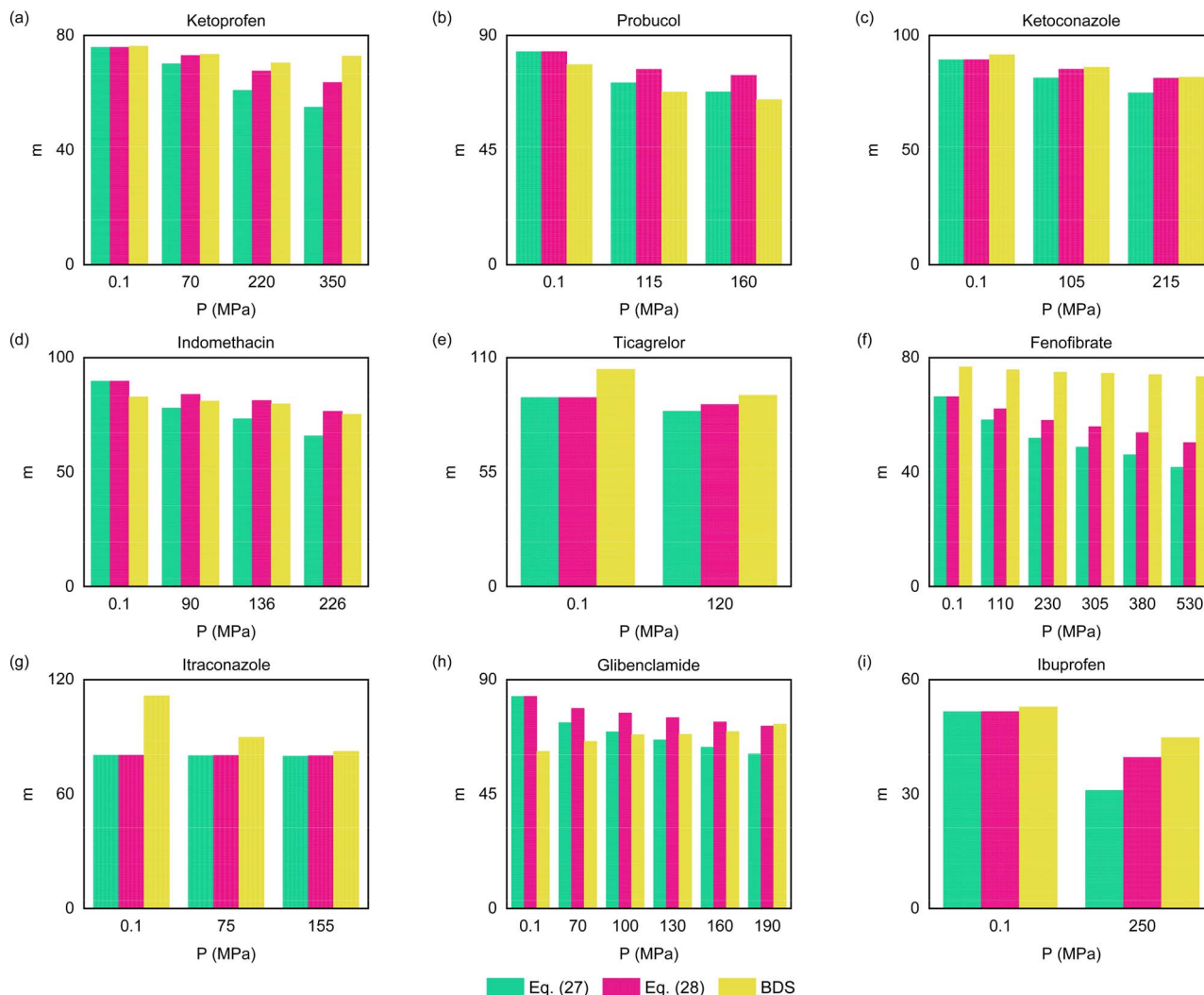


Fig. 4 (Color online) The correlation between the dynamic fragility and the hydrostatic pressure in the case of (a) ketoprofen, (b) probucol, (c) ketoconazole, (d) indomethacin, (e) ticagrelor, (f) fenofibrate, (g) itraconazole, (h) glibenclamide, and (i) ibuprofen. Whereas green columns are built from eqn (27), pink ones are constructed from eqn (28). Yellow columns indicate BDS data gathered from Ref. 114 and 131–138 (see Table S1 in the ESI†).

and cause the sample to be more fragile. Yet, it is clear to see that eqn (28) outperforms eqn (27) in predicting the magnitude of  $m$ . Replacing eqn (27) with (28) can narrow the gap between ECNLE analyses and BDS measurements by a factor of 1.1 to 16.0 while preserving the required computational efficiency. It should be stressed that accurate information about  $m$  is indispensable for controlling the crystallization tendency of pharmaceuticals.<sup>51</sup> Based on the specific value of  $m$ , we can divide amorphous drugs into three principal groups: strong ( $m \leq 30$ ), intermediate ( $30 < m < 100$ ), and fragile ( $m \geq 100$ ).<sup>142</sup> Modern experiments and simulations suggest that the smaller the fragility, the greater the stability.<sup>96–98</sup> In that context, our simple but effective toolkit would be practically meaningful for developing tableting processes, where relevant glass-forming systems are often compressed to hundreds of megapascals and forced to undergo dramatic changes in dynamic fragility.<sup>36</sup>

Another appealing aspect to discuss is that the difference between ECNLE and BDS data remains relatively large for

fenofibrate<sup>135</sup> despite a substantial improvement in the chemical mapping of this substance. At  $P = 530$  MPa, we obtain  $m = 41.75$  from eqn (27) and  $m = 50.32$  from eqn (28). Meanwhile, using the BDS technique brings  $m = 73.3$ .<sup>135</sup> In our opinion, there are two primary reasons behind this problem.

First, accurately determining the dynamic fragility of soft materials is a daunting task for experimentalists.<sup>93</sup> The evidence is that the reported experimental results for  $m$  are frequently accompanied by enormous error bars due to the non-Arrhenius nature of supercooled liquids.<sup>131,137</sup> Moreover, this physical quantity will experience a sharp fluctuation if experimentalists apply different fitting methods to analyze their dataset.<sup>135</sup> In the case of fenofibrate, the measured value of  $m$  ranges from 76 to 94, even when the applied pressure is merely about 0.1 MPa.<sup>148–151</sup> More efforts are necessary to deal with the mentioned predicament.

Second, the hydrogen-bond network of fenofibrate may strongly affect its glassy dynamics.<sup>135</sup> As shown by Grzybowska





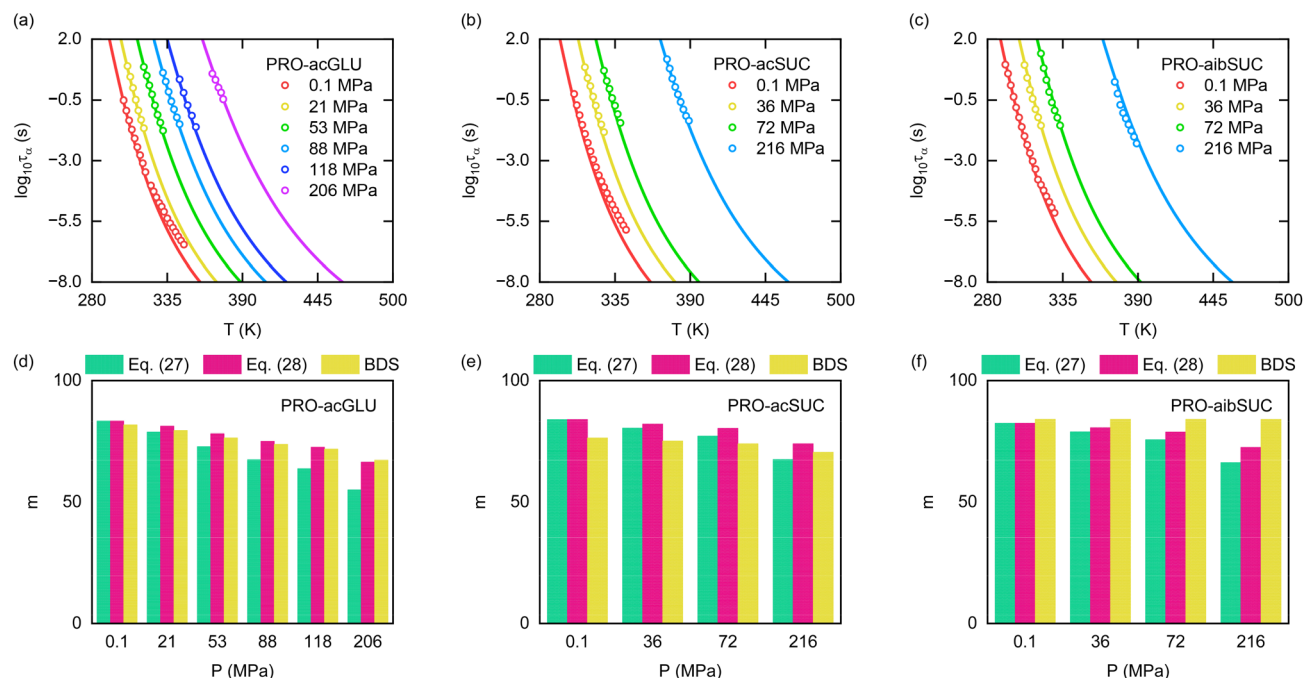


Fig. 5 (Color online) The first row: ECNLE analyses (solid lines) and BDS measurements<sup>160</sup> (open circles) for the structural relaxation time of probucol-based mixtures, including (a) PRO-acGLU, (b) PRO-acSUC, and (c) PRO-aibSUC. The second row: compression effects on the dynamic fragility of (d) PRO-acGLU, (e) PRO-acSUC, and (f) PRO-aibSUC obtained from the previous chemical mapping (green columns), the present macroscopic approach (pink columns), and the BDS experimental method<sup>160</sup> (yellow columns).

*et al.*,<sup>51</sup> whereas vdW interactions favor the decline of  $m$ ,<sup>152</sup> hydrogen bonds do the opposite.<sup>153</sup> That means we should concurrently combine microscopic and macroscopic ECNLE approaches to acquire better predictions of fenofibrate. The combination is expected to occur as follows. If the intermolecular potential of fenofibrate is known, we can derive its radial distribution function and static structure factor from the standard reference interaction site model.<sup>154–156</sup> Then, it is possible to recalculate local and collective barriers *via* the projectionless dynamics theory.<sup>157–159</sup> The last step is to add  $P$ - $T$  contributions to ECNLE outputs *via* our newly developed chemical mapping. We believe this is one of the most viable strategies for capturing molecular dynamics in amorphous fenofibrate on the theoretical side. Nevertheless, it would involve a lot of sophisticated computational techniques. Thus, this fascinating subject deserves consideration in a separate ECNLE study.

After obtaining encouraging outcomes for single-component amorphous drugs, a natural question arises: Is our ECNLE theory applicable to more complex pharmaceutical systems? To answer this question, we perform additional calculations for three homogenous solid dispersions constituted of probucol and acetylated saccharide with a molar ratio of 5 : 1, including PRO-acGLU ( $k_1 = 292.71$  K,  $k_2 = 2.99$ ,  $k_3 = 709.81$  MPa), PRO-acSUC ( $k_1 = 294.72$  K,  $k_2 = 1.97$ ,  $k_3 = 774.68$  MPa), and PRO-aibSUC ( $k_1 = 289.43$  K,  $k_2 = 1.95$ ,  $k_3 = 744.25$  MPa).<sup>160,161</sup> The glass transition of these binary mixtures is supposed to happen at  $\phi_g = 0.61095$ , similar to pure probucol.<sup>132</sup> As illustrated in Fig. 5, our theoretical model can quantitatively explain experimental observations<sup>160</sup> on the glassy dynamics of PRO-acGLU,

PRO-acSUC, and PRO-aibSUC without heavy computational workloads. Regarding the structural relaxation time, ECNLE curves pass through most BDS benchmarks<sup>160</sup> regardless of low or high pressures. Regarding the dynamic fragility, the maximum error between eqn (28) and BDS data<sup>160</sup> is 2.24% for PRO-acGLU, 9.75% for PRO-acSUC, and 13.57% for PRO-aibSUC. These figures are experimentally acceptable because  $m$  is considered the most sensitive quantity in soft-matter physics.<sup>93</sup> It is more remarkable that the above agreements do not involve any adjustable parameters. Therefore, our ECNLE theory has great potential for decoding the mystery of multi-component amorphous drugs and extending their practical applicability to health protection and promotion.

## 4. Effects of kinetic vitrification

Having successfully explored the high-pressure region, we turn our attention to the low-temperature area. It is well known that the  $V$ - $T$  line exhibits an abrupt change in its average steepness at the glass transition point.<sup>52</sup> This event implies that we should replace  $\beta_T$  with  $\beta_T - \Delta\beta_T$  in our chemical mapping to appropriately describe the molecular mobility of amorphous drugs at  $T < T_g$ . The key parameter here is  $\Delta\beta_T$ , which characterizes the influences of kinetic vitrification on thermal expansion ( $\Delta\beta_T > 0$ ). So, how is  $\Delta\beta_T$  determined? The answer lies in a similarity between vitrified and dislocated materials.

A substantial body of evidence shows that crystals tend to behave like glasses when line defects appear in their lattice structures.<sup>162–164</sup> For example, Bako *et al.*<sup>165</sup> observed the aging



phenomenon – a hallmark of glassy dynamics – in the correlation function and the diffusion coefficient of dislocations *via* mesoscale simulations. Based on local mechanical perturbation experiments, Gerbode *et al.*<sup>166</sup> found that the relaxation of dislocations in degenerate crystals would undergo two stages – caging and hopping – similar to what happens in glass-forming liquids. A remarkable analogy between defective and glassy dynamics was also recorded in the recent studies of Ispanovity *et al.*,<sup>167</sup> Lehtinen *et al.*,<sup>168</sup> and Ovaska *et al.*<sup>169</sup> on the plastic deformation of crystalline solids in two- and three-dimensional spaces. In particular, Burakovsky *et al.*<sup>170–172</sup> discovered that the melting process of elements could be seen as a defect-mediated structural transformation, where half of the particles were in a dislocation core. This discovery gave them<sup>170–172</sup>

$$\frac{G_m V_m}{T_m} = C_m, \quad (29)$$

where  $C_m$  was a universal constant,  $G_m$  was the shear modulus, and  $V_m$  was the molecular volume at the melting temperature  $T_m$ . Excitingly, the Burakovsky criterion<sup>170–172</sup> for melting transition is identical to our ECNLE criterion for glass transition, even though they have different theoretical backgrounds. The perfect symmetry between eqn (17) and (29) reaffirms that vitrified and dislocated materials are strongly correlated. Hence, we can utilize available knowledge of line defects in crystallography to address thorny issues about amorphous drugs in the field of soft matter.

To be more specific, we consider a faulty crystal with physical properties summarized in Fig. 6. Initially, our system exists at the Kauzmann point ( $V_K, T_K$ ), where the  $V$ - $T$  profiles of solid and liquid phases cross each other.<sup>173</sup> Then, it is isobarically heated to the critical location ( $V_m, T_m$ ) on the  $V$ - $T$  diagram. This thermodynamic path is modeled by

$$V_m = V_K[1 + \beta_m(T_m - T_K)], \quad (30)$$

where  $\beta_m$  is the volumetric expansivity of the crystalline phase. If we continue to supply thermal energy to the sample, it will be liquified. This process is characterized by the fusion volume

$\Delta V_m$  and the fusion enthalpy  $\Delta H_m$ . These quantities are closely related, as shown by the Clausius–Clapeyron formula,<sup>174,175</sup>

$$\Delta V_m = \frac{\Delta H_m}{T_m} \frac{dT_m}{dP}. \quad (31)$$

Besides, the liquefaction of lattice spaces is mainly driven by the proliferation of dislocations, so the latent heat of fusion can be straightforwardly estimated *via* the enthalpy of defect formation as<sup>170–172</sup>

$$\Delta H_m = \frac{C_m}{8\pi} T_m. \quad (32)$$

Another thing to note is that the thermal expansion coefficient climbs from  $\beta_m$  to  $\beta_m + \Delta\beta_m$  upon melting. Thus, we have

$$V_m + \Delta V_m = V_K[1 + (\beta_m + \Delta\beta_m)(T_m - T_K)]. \quad (33)$$

Combining eqn (30)–(33) yields

$$\Delta\beta_m = \frac{C_m}{8\pi V_K(T_m - T_K)} \frac{dT_m}{dP}. \quad (34)$$

Relying on the resemblance between melting and glass transitions mentioned earlier, we can expect that  $\Delta\beta_m$  and  $\Delta\beta_T$  have the same analytical form. Accordingly, when returning to amorphous pharmaceuticals, we obtain.

$$\Delta\beta_T = \frac{C_g}{8\pi V_K(T_g - T_K)} \frac{dT_g}{dP}. \quad (35)$$

It is easy to see from eqn (8) that  $T_K$  is associated with  $T_g$  *via*

$$T_K = T_g - \frac{\phi_K - \phi_g}{\beta_T \phi_0}, \quad (36)$$

where  $\phi_K = 0.67233$  is determined by parameterizing ECNLE data for  $\tau_\alpha$  in Table 1 with the Vogel–Fulcher–Tammann function<sup>176</sup> at  $\phi > 0.55$ . Inserting eqn (36) into (35) provides

$$\Delta\beta_T = \frac{C_g \phi_0}{8\pi(\phi_K - \phi_g)} \frac{\beta_T}{V_K} \frac{dT_g}{dP}. \quad (37)$$

Eqn (37) takes a central position in accessing the glassy state *via* the ECNLE theory. In the  $P \rightarrow 0$  limit, its mathematical expression is simplified by

$$\Delta\beta_T = 0.3951 \frac{k_B}{V_K} \frac{dT_g}{dP}. \quad (38)$$

To save time and cost, we can approximate  $V_K$  as the measured volume of the crystalline phase. The error of this approximation is only a few percent because the thermal expansivity of crystals is quite low<sup>177</sup> ( $\beta_m = 10^{-6}$ – $10^{-4}$  K<sup>-1</sup>) and the Kauzmann temperature<sup>178</sup> ( $T_K = 100$ – $600$  K) is not too far from the reported temperature in crystallographic<sup>179</sup> ( $T = 100$ – $400$  K).

To demonstrate how well our strategy works, we apply eqn (38) to carvedilol ( $T_g = 310$  K), nimesulide ( $T_g = 291$  K), paracetamol ( $T_g = 297$  K), and probucol ( $T_g = 293.8$  K), whose  $\alpha$ -relaxation behaviors were unambiguously reported at low temperatures. Their volume can be readily found in the Cambridge Structural Database.<sup>179</sup> Note that the parameter  $V_K$  is affected by polymorphic effects. Based on the melting point

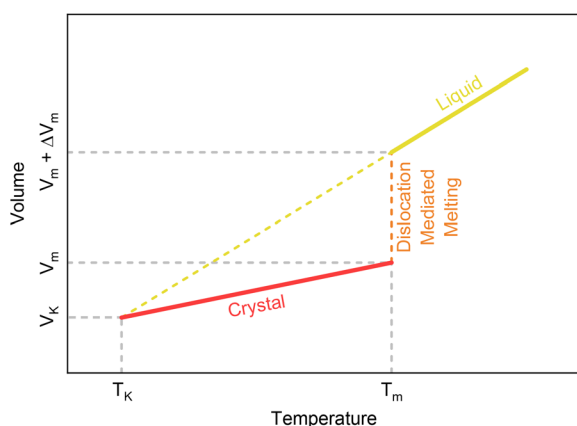
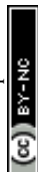


Fig. 6 (Color online) The phase diagram of the defective structure used to calculate  $\Delta\beta_T$ .



**Table 3** The molecular volume and the glass-transition slope of the investigated active pharmaceutical ingredients

Drug	$V_K$ ( $\text{\AA}^3$ )	$dT_g/dP$ (K MPa $^{-1}$ )	Reference
Carvedilol	2116.8	0.16	183 and 185
Nimesulide	2663.4	0.24	180 and 186
Paracetamol	1500.2	0.24	181, 187 and 188
Probuco	3116.0	0.44	132 and 182

reported in the ESI,<sup>†</sup> we determine  $V_K$  using nimesulide form I,<sup>180</sup> paracetamol form II,<sup>181</sup> and probuocol form I.<sup>182</sup> For carvedilol, we do not know which polymorph was amorphized in earlier BDS experiments.<sup>51</sup> Yet, since the  $V_K$  value of carvedilol weakly depends on its polymorphism,<sup>183</sup> we employ form II to construct the chemical mapping. This crystalline structure is widely used in marketed formulations due to its faster dissolution at bio-relevant pH levels.<sup>184</sup>

In addition, it is practicable to directly extract the initial gradient of glass-liquid boundaries from prior BDS or PVT measurements.<sup>132,185,186</sup> For paracetamol, because information about glassy dynamics at elevated pressures is unavailable, we employ the non-equilibrium thermodynamic approximation of Lima *et al.*<sup>187</sup> to the differential-scanning calorimetry data of Ledru *et al.*<sup>188</sup> to infer  $dT_g/dP$  from  $dT_m/dP$ . All experimental inputs we require are detailed in Table 3. On that basis, we figure out  $\Delta\beta_T = 4.1232 \times 10^{-4} \text{ K}^{-1}$  for carvedilol,  $\Delta\beta_T = 4.9154 \times 10^{-4} \text{ K}^{-1}$  for nimesulide,  $\Delta\beta_T = 8.7268 \times 10^{-4} \text{ K}^{-1}$  for paracetamol, and  $\Delta\beta_T = 7.7028 \times 10^{-4} \text{ K}^{-1}$  for probuocol. These numbers are in good accordance with recent experiments on the equation of state of glass-forming drugs.<sup>185</sup>

Fig. 7 shows finite-temperature effects on the structural relaxation time of carvedilol and nimesulide. Generally, there is a sudden switch in their molecular dynamics from super-Arrhenius to Arrhenius-like types near the vitrification point. This strange event is called dynamic decoupling – one of the most elusive phenomena in soft-matter physics.<sup>189</sup> However, our ECNLE theory can reliably predict complex changes in relaxation maps by updating the chemical mapping with eqn (37) and (38). It is conspicuous that ECNLE calculations perfectly match BDS measurements<sup>51,190</sup> in the supercooled region. After adding  $\Delta\beta_T$  to  $\beta_T$ , they can even reproduce MPC results<sup>51,190</sup> in the glassy area with considerable accuracy. As far as we know, no theoretical or computational methods can satisfactorily explain the primary relaxation of carvedilol and nimesulide from pico-second to terasecond timescales without fitting parameters, except for the ECNLE. These positive outcomes validate the effectiveness of our strategy.

Notably, before introducing a new medicine to the market, one has to check whether its relaxation time exceeds three years under ambient conditions ( $P = 0.1 \text{ MPa}$  and  $T = 293 \text{ K}$ ).<sup>36</sup> This number is the minimum self-lifetime needed for commercial pharmaceutical products. As illustrated in Fig. 7, none of the studied amorphous drugs meet the above requirement because of the decoupling phenomenon. If we ignore the jump of thermal expansivity near the glass transition, we will overestimate  $\tau_\alpha$  by several orders of magnitude and misjudge the

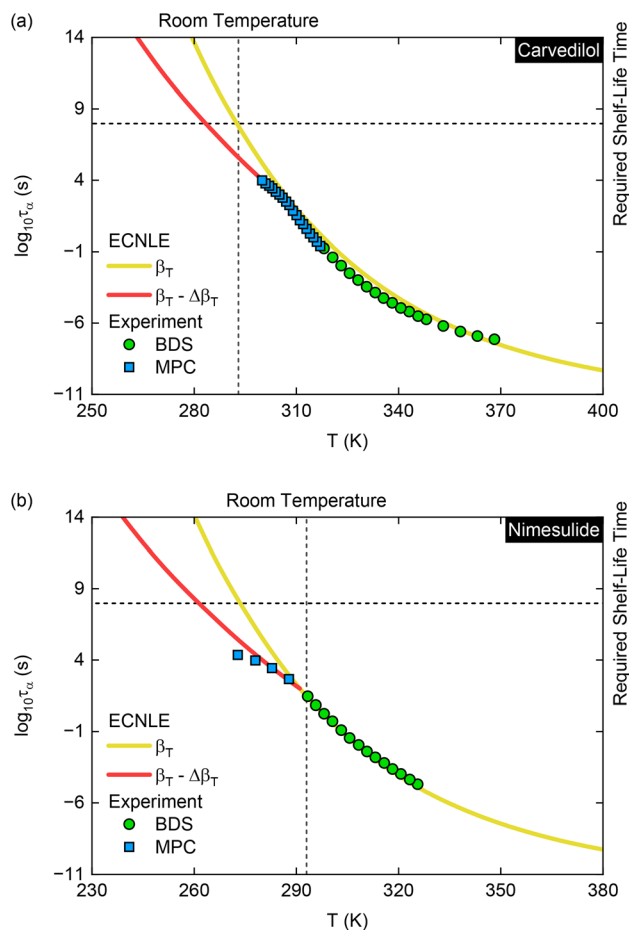


**Fig. 7** (Color online) (a) ECNLE and BDS/MPC<sup>51</sup> predictions of the  $\alpha$  relaxation map of carvedilol in supercooled and vitrified states. (b) The structural relaxation time of nimesulide above and below its glass transition temperature derived from ECNLE and BDS/MPC<sup>190</sup> methods.

practical applicability of carvedilol and nimesulide. More attempts are necessitated to reinforce their physical stability before commercialization. Using polymeric precipitation inhibitors (*e.g.*, cellulose<sup>191</sup> or polyvinylpyrrolidone<sup>190</sup>) may be a fruitful avenue for actualizing the potential of amorphous carvedilol and nimesulide in disease prevention and treatment.

Fig. 8 presents the  $\alpha$  relaxation map of paracetamol and probuocol. Fundamentally, our ECNLE theory still works very well. All BDS and MPC information<sup>132,192,193</sup> is quantitatively decoded regardless of high or low temperatures. In particular, the structural relaxation time  $\tau_\alpha$  of paracetamol can be utilized to predict its recrystallization time  $\tau_{cr}$  *via*<sup>194</sup>

$$\log_{10} \tau_{cr}[\text{h}] = 0.4861 \log_{10} \left( \frac{\tau_\alpha[\text{s}]}{T[\text{K}]} \right) + 3.0208. \quad (39)$$

At  $T_g/T = 1.0683$ , recent differential-scanning-calorimetry measurements<sup>194</sup> reveal that amorphous paracetamol samples would recrystallize after 2319 h, comparable to  $\tau_{cr} = 3654 \text{ h}$  deduced from ECNLE analyses in the glassy state. This emphasizes the pivotal role of  $\alpha$  processes in controlling the physical stability of glass-forming drugs.



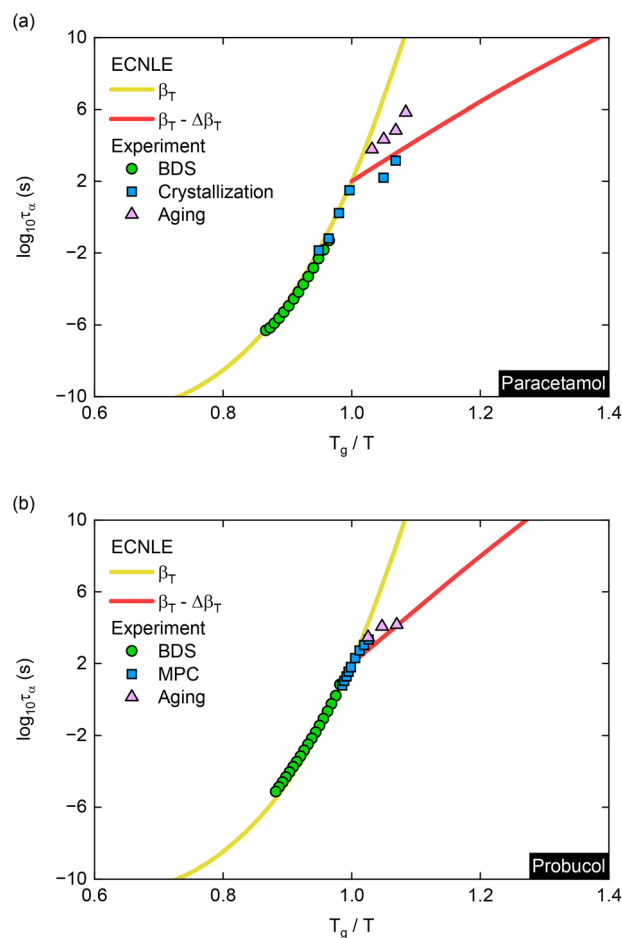


Fig. 8 (Color online) (a) Theoretical and experimental<sup>193,194</sup> outcomes for the structural relaxation process of paracetamol in the amorphous form. (b) Calculated and measured<sup>132,192,195</sup> data for the primary relaxation time of probucol after amorphization.

Another aspect worth mentioning is that ECNLE calculations markedly differ from aging experiments.<sup>194,195</sup> At  $T_g/T = 1.0255$ , aging data for probucol is  $\tau_{\alpha} = 0.81$  h,<sup>195</sup> about fivefold longer than the ECNLE counterpart ( $\tau_{\alpha} = 0.16$  h). That is because we neglect the time dependence of  $\Delta\beta_T$ . After passing through the vitrification point, the thermal expansivity of amorphous pharmaceuticals abruptly drops from  $\beta_T$  to  $\beta_T - \Delta\beta_T$ .<sup>52</sup> Nevertheless, this physical quantity tends to return to its original value during aging.<sup>196</sup> In other words, the older the sample gets, the weaker the decoupling becomes. Although the above principle sounds very simple, dealing with aging-related problems is a major challenge for physicists.<sup>197–200</sup> One of the most prominent reasons is that aging effects can significantly delay the decoupling event. As shown in the case of paracetamol, old systems begin exhibiting Arrhenius-like behaviors at  $\tau_{\alpha} = 1.83$  h,<sup>194</sup> much later than the commencement of dynamic decoupling in fresh samples ( $\tau_{\alpha} = 0.03$  h). What is the underlying mechanism behind this enigmatic phenomenon? How do we locate the decoupling position of amorphous drugs on the relaxation diagram over time? Are dislocation glasses the key we

are looking for? These intriguing questions will be the subject of ECNLE research in the future.

## 5. Conclusion

Inspired by the ECNLE theory, we have formulated a time-saving, cost-effective, and user-friendly macroscopic approach to shed light on the influences of hydrostatic compression and kinetic vitrification on the molecular dynamics of amorphous drugs. This free-of-adjustable-parameter method has helped us decipher most BDS and MPC observations on  $\alpha$  relaxation processes without computational burdens. Additionally, our ECNLE calculations have unveiled some interesting relations between thermodynamic and elastic properties, between melting and glass transitions, and between crystalline and non-crystalline solids. To facilitate further projects, we have presented all physical pictures, computational steps, and numerical results as clearly as possible. Some viable ideas to extend our theoretical model have also been given. Therefore, we are eager to witness new scientific advances in amorphous drugs in the foreseeable future.

## Data availability

The authors declare that the data supporting the findings of this study are available within the paper.

## Author contributions

Tran Dinh Cuong: conceptualization, methodology, investigation, writing – original draft, writing – review & editing, visualization. Anh D. Phan: resources, supervision.

## Conflicts of interest

The authors declare that they have no known competing financial interests or personal relationships that could have appeared to influence the work reported in this paper.

## Acknowledgements

This research was funded by the Vietnam National Foundation for Science and Technology Development (NAFOSTED) under Grant No. 103.01-2023.62.

## References

- 1 M. A. Spyrou, K. I. Bos, A. Herbig and J. Krause, Ancient pathogen genomics as an emerging tool for infectious disease research, *Nat. Rev. Genet.*, 2019, **20**, 323.
- 2 N. Rascovan, K. G. Sjogren, K. Kristiansen, R. Nielsen, E. Willerslev, C. Desnues and S. Rasmussen, Emergence and spread of basal lineages of *Yersinia pestis* during the Neolithic decline, *Cell*, 2019, **176**, 295.
- 3 F. Maixner, B. Krause-Kyora, D. Turaev, A. Herbig, M. R. Hoopmann, J. L. Hallows, U. Kusebauch, E. E. Vigl, P. Malfertheiner, F. Megraud, N. O'Sullivan, G. Cipollini,





- V. Coia, M. Samadelli, L. Engstrand, B. Linz, R. L. Moritz, R. Grimm, J. Krause, A. Nebel, *et al.*, The 5300-year-old *Helicobacter pylori* genome of the Iceman, *Science*, 2016, **351**, 162.
- 4 B. Muhlemann, T. C. Jones, P. D. B. Damgaard, M. E. Allentoft, I. Shevnina, A. Logvin, E. Usmanova, I. P. Panyushkina, B. Boldgiv, T. Bazartseren, K. Tashbaeva, V. Merz, N. Lau, V. Smrcka, D. Voyakin, E. Kitov, A. Epimakhov, D. Pokutta, M. Vicze, T. D. Price, *et al.*, Ancient hepatitis B viruses from the Bronze Age to the Medieval period, *Nature*, 2018, **557**, 418.
  - 5 B. Muhlemann, A. Margaryan, P. D. B. Damgaard, M. E. Allentoft, L. Vinner, A. J. Hansen, A. Weber, V. I. Bazaliiskii, M. Molak, J. Arneborg, W. Bogdanowicz, C. Falys, M. Sablin, V. Smrcka, S. Sten, K. Tashbaeva, N. Lynnerup, M. Sikora, D. J. Smith, R. A. M. Fouchier, *et al.*, Ancient human parvovirus B19 in Eurasia reveals its long-term association with humans, *Proc. Natl. Acad. Sci. U. S. A.*, 2018, **115**, 7557.
  - 6 D. M. Wagner, J. Klunk, M. Harbeck, A. Devault, N. Waglechner, J. W. Sahl, J. Enk, D. N. Birdsell, M. Kuch, C. Lumibao, D. Poinar, T. Pearson, M. Fourment, B. Golding, J. M. Riehm, D. J. D. Earn, S. DeWitte, J. M. Rouillard, G. Grupe, I. Wiechmann, *et al.*, *Yersinia pestis* and the plague of Justinian 541–543 AD: A genomic analysis, *Lancet Infect. Dis.*, 2014, **14**, 319.
  - 7 M. A. Spyrou, L. Musralina, G. A. G. Ruscone, A. Kocher, P. G. Borbone, V. I. Khartanovich, A. Buzhilova, L. Djansugurova, K. I. Bos, D. Kuhnert, W. Haak, P. Slavin and J. Krause, The source of the Black Death in fourteenth-century central Eurasia, *Nature*, 2022, **606**, 718.
  - 8 M. Worobey, T. D. Watts, R. A. McKay, M. A. Suchard, T. Granade, D. E. Teuwen, B. A. Koblin, W. Heneine, P. Lemey and H. W. Jaffe, 1970s and 'Patient 0' HIV-1 genomes illuminate early HIV/AIDS history in North America, *Nature*, 2016, **539**, 98.
  - 9 E. C. Holmes, G. Dudas, A. Rambaut and K. G. Andersen, The evolution of Ebola virus: Insights from the 2013–2016 epidemic, *Nature*, 2016, **538**, 193.
  - 10 J. Li, S. Lai, G. F. Gao and W. Shi, The emergence, genomic diversity and global spread of SARS-CoV-2, *Nature*, 2021, **600**, 408.
  - 11 P. Piot, M. Bartos, P. D. Ghys, N. Walker and B. Schwartlander, The global impact of HIV/AIDS, *Nature*, 2001, **410**, 968.
  - 12 W. Msemburi, A. Karlinsky, V. Knutson, S. Aleshin-Guendel, S. Chatterji and J. Wakefield, The WHO estimates of excess mortality associated with the COVID-19 pandemic, *Nature*, 2023, **613**, 130.
  - 13 L. Li, A. Taeihagh and S. Y. Tan, A scoping review of the impacts of COVID-19 physical distancing measures on vulnerable population groups, *Nat. Commun.*, 2023, **14**, 599.
  - 14 X. Lin, Y. Xu, X. Pan, J. Xu, Y. Ding, X. Sun, X. Song, Y. Ren and P. F. Shan, Global, regional, and national burden and trend of diabetes in 195 countries and territories: An analysis from 1990 to 2025, *Sci. Rep.*, 2020, **10**, 14790.
  - 15 G. A. Roth, G. A. Mensah, C. O. Johnson, G. Addolorato, E. Ammirati, L. M. Baddour, N. C. Barengo, A. Z. Beaton, E. J. Benjamin, C. P. Benziger, A. Bonny, M. Brauer, M. Brodmann, T. J. Cahill, J. Carapetis, A. L. Catapano, S. S. Chugh, L. T. Cooper, J. Coresh, M. Criqui, *et al.*, Global burden of cardiovascular diseases and risk factors, 1990–2019: Update from the GBD 2019 study, *J. Am. Coll. Cardiol.*, 2020, **76**, 2982.
  - 16 A. Leiter, R. R. Veluswamy and J. P. Wisnivesky, The global burden of lung cancer: Current status and future trends, *Nat. Rev. Clin. Oncol.*, 2023, **20**, 624.
  - 17 World Health Organization, Cardiovascular diseases (CVDs), [https://www.who.int/news-room/fact-sheets/detail/cardiovascular-diseases-\(cvds\)](https://www.who.int/news-room/fact-sheets/detail/cardiovascular-diseases-(cvds)), accessed May 7, 2024.
  - 18 S. Mendis and V. Fuster, National policies and strategies for noncommunicable diseases, *Nat. Rev. Cardiol.*, 2009, **6**, 723.
  - 19 M. Ezzati, J. Pearson-Stuttard, J. E. Bennett and C. D. Mathers, Acting on non-communicable diseases in low- and middle-income tropical countries, *Nature*, 2018, **559**, 507.
  - 20 J. L. Excler, M. Saville, S. Berkley and J. H. Kim, Vaccine development for emerging infectious diseases, *Nat. Med.*, 2021, **27**, 591.
  - 21 A. G. Atanasov, S. B. Zotchev, V. M. Dirsch, International Natural Product Sciences Taskforce and C. T. Supuran, Natural products in drug discovery: Advances and opportunities, *Nat. Rev. Drug Discovery*, 2021, **20**, 200.
  - 22 J. Vamathevan, D. Clark, P. Czodrowski, I. Dunham, E. Ferran, G. Lee, B. Li, A. Madabhushi, P. Shah, M. Spitzer and S. Zhao, Applications of machine learning in drug discovery and development, *Nat. Rev. Drug Discovery*, 2019, **18**, 463.
  - 23 A. R. Kirtane, M. Verma, P. Karandikar, J. Furin, R. Langer and G. Traverso, Nanotechnology approaches for global infectious diseases, *Nat. Nanotechnol.*, 2021, **16**, 369.
  - 24 T. Li and A. Mattei, *Pharmaceutical Crystals: Science and Engineering*, Wiley, Hoboken, 2019.
  - 25 S. R. Vippagunta, H. G. Brittain and D. J. W. Grant, Crystalline solids, *Adv. Drug Delivery Rev.*, 2001, **48**, 3.
  - 26 S. Datta and D. J. W. Grant, Crystal structures of drugs: Advances in determination, prediction and engineering, *Nat. Rev. Drug Discovery*, 2004, **3**, 42.
  - 27 D. L. Hughes, Review of synthetic routes and crystalline forms of the antiandrogen oncology drugs enzalutamide, apalutamide, and darolutamide, *Org. Process Res. Dev.*, 2020, **24**, 347.
  - 28 D. L. Hughes, Review of synthetic routes and crystalline forms of the oncology drugs capmatinib, seliperatinib, and pralsetinib, *Org. Process Res. Dev.*, 2021, **25**, 2192.
  - 29 L. Di, P. V. Fish and T. Mano, Bridging solubility between drug discovery and development, *Drug Discovery Today*, 2012, **17**, 486.
  - 30 H. D. Williams, N. L. Trevaskis, S. A. Charman, R. M. Shanker, W. N. Charman, C. W. Pouton and C. J. H. Porter, Strategies to address low drug solubility in discovery and development, *Pharmacol. Rev.*, 2013, **65**, 315.



- 31 S. Kalepu and V. Nekkanti, Insoluble drug delivery strategies: Review of recent advances and business prospects, *Acta Pharm. Sin. B*, 2015, **5**, 442.
- 32 J. B. Dressman and C. Reppas, *Oral Drug Absorption: Prediction and Assessment*, CRC Press, Boca Raton, 2016.
- 33 Q. Ma, C. Wang, X. Li, H. Guo, J. Meng, J. Liu and H. Xu, Fabrication of water-soluble polymer-encapsulated As<sub>4</sub>S<sub>4</sub> to increase oral bioavailability and chemotherapeutic efficacy in AML mice, *Sci. Rep.*, 2016, **6**, 29348.
- 34 J. K. Aronson, *Meyler's Side Effects of Drugs: the International Encyclopedia of Adverse Drug Reactions and Interactions*, Elsevier, Oxford, 2016.
- 35 A. O. Iuga and M. J. McGuire, Adherence and health care costs, *Risk Manag. Healthc. Policy*, 2014, **7**, 35.
- 36 M. Rams-Baron, R. Jachowicz, E. Boldyreva, D. Zhou, W. Jamroz, and M. Paluch, *Amorphous Drugs: Benefits and Challenges*, Springer, Heidelberg, 2018.
- 37 J. F. Willart and M. Descamps, Solid state amorphization of pharmaceuticals, *Mol. Pharm.*, 2008, **5**, 905.
- 38 A. Alzahrani, D. Nyavanandi, P. Mandati, A. A. A. Youssef, S. Narala, S. Bandari and M. Repka, A systematic and robust assessment of hot-melt extrusion-based amorphous solid dispersions: Theoretical prediction to practical implementation, *Int. J. Pharm.*, 2022, **624**, 121951.
- 39 S. Qi and D. Craig, Recent developments in micro- and nanofabrication techniques for the preparation of amorphous pharmaceutical dosage forms, *Adv. Drug Delivery Rev.*, 2016, **100**, 67.
- 40 J. F. Willart, A. De Gussemme, S. Hemon, M. Descamps, F. Leveiller and A. Rameau, Vitrification and polymorphism of trehalose induced by dehydration of trehalose dihydrate, *J. Phys. Chem. B*, 2002, **106**, 3365.
- 41 S. J. Dengale, O. P. Ranjan, S. S. Hussien, B. S. M. Krishna, P. B. Musmade, G. G. Shenoy and K. Bhat, Preparation and characterization of co-amorphous ritonavir-indomethacin systems by solvent evaporation technique: Improved dissolution behavior and physical stability without evidence of intermolecular interactions, *Eur. J. Pharm. Sci.*, 2014, **62**, 57.
- 42 B. C. Hancock and M. Parks, What is the true solubility advantage for amorphous pharmaceuticals?, *Pharm. Res.*, 2000, **17**, 397.
- 43 S. B. Murdande, M. J. Pikal, R. M. Shanker and R. H. Bogner, Solubility advantage of amorphous pharmaceuticals: I. A thermodynamic analysis, *J. Pharm. Sci.*, 2010, **99**, 1254.
- 44 S. B. Murdande, M. J. Pikal, R. M. Shanker and R. H. Bogner, Solubility advantage of amorphous pharmaceuticals: II. Application of quantitative thermodynamic relationships for prediction of solubility enhancement in structurally diverse insoluble pharmaceuticals, *Pharm. Res.*, 2010, **27**, 2704.
- 45 R. Paus, Y. Ji, L. Vahle and G. Sadowski, Predicting the solubility advantage of amorphous pharmaceuticals: A novel thermodynamic approach, *Mol. Pharm.*, 2015, **12**, 2823.
- 46 V. H. Thomas, S. Bhattachar, L. Hitchingham, P. Zocharski, M. Naath, N. Surendran, C. L. Stoner and A. El-Kattan, The road map to oral bioavailability: An industrial perspective, *Expert Opin. Drug Metab. Toxicol.*, 2006, **2**, 591.
- 47 C. Bhugra, R. Shmeis, S. L. Krill and M. J. Pikal, Prediction of onset of crystallization from experimental relaxation times. II. Comparison between predicted and experimental onset times, *J. Pharm. Sci.*, 2008, **97**, 455.
- 48 B. V. Eerdenbrugh, J. A. Baird and L. S. Taylor, Crystallization tendency of active pharmaceutical ingredients following rapid solvent evaporation — Classification and comparison with crystallization tendency from under cooled melts, *J. Pharm. Sci.*, 2010, **99**, 3826.
- 49 K. Kawakami, T. Harada, K. Miura, Y. Yoshihashi, E. Yonemochi, K. Terada and H. Moriyama, Relationship between crystallization tendencies during cooling from melt and isothermal storage: Toward a general understanding of physical stability of pharmaceutical glasses, *Mol. Pharm.*, 2014, **11**, 1835.
- 50 J. Sibik, K. Lobmann, T. Rades and J. A. Zeitler, Predicting crystallization of amorphous drugs with terahertz spectroscopy, *Mol. Pharm.*, 2015, **12**, 3062.
- 51 K. Grzybowska, S. Capaccioli and M. Paluch, Recent developments in the experimental investigations of relaxations in pharmaceuticals by dielectric techniques at ambient and elevated pressure, *Adv. Drug Delivery Rev.*, 2016, **100**, 158.
- 52 J. Knapik-Kowalczyk, M. Rams-Baron and M. Paluch, Current research trends in dielectric relaxation studies of amorphous pharmaceuticals: Physical stability, tautomerism, and the role of hydrogen bonding, *Trends Anal. Chem.*, 2021, **134**, 116097.
- 53 K. Adrjanowicz, K. Kaminski, Z. Wojnarowska, M. Dulski, L. Hawelek, S. Pawlus, M. Paluch and W. Sawicki, Dielectric relaxation and crystallization kinetics of ibuprofen at ambient and elevated pressure, *J. Phys. Chem. B*, 2010, **114**, 6579.
- 54 Z. Wojnarowska, L. Hawelek, M. Paluch, W. Sawicki and K. L. Ngai, Molecular dynamics at ambient and elevated pressure of the amorphous pharmaceutical: Nonivamide (pelargonic acid vanillylamide), *J. Chem. Phys.*, 2011, **134**, 044517.
- 55 M. Rams-Baron, J. Pacuła, A. Jedrzejowska, J. Knapik-Kowalczyk and M. Paluch, Changes in physical stability of supercooled etoricoxib after compression, *Mol. Pharm.*, 2018, **15**, 3969.
- 56 A. Minecka, E. Kaminska, D. Heczko, K. Jurkiewicz, K. Wolnica, M. Dulski, B. Hachula, W. Pisarski, M. Tarnacka, A. Talik, K. Kaminski and M. Paluch, Studying structural and local dynamics in model H-bonded active ingredient — Curcumin in the supercooled and glassy states at various thermodynamic conditions, *Eur. J. Pharm. Sci.*, 2019, **135**, 38.
- 57 K. Chmiel, J. Knapik-Kowalczyk and M. Paluch, How does the high pressure affects the solubility of the drug within



- the polymer matrix in solid dispersion systems, *Eur. J. Pharm. Biopharm.*, 2019, **143**, 8.
- 58 K. Grzybowska, M. Paluch, A. Grzybowski, Z. Wojnarowska, L. Hawelek, K. Kolodziejczyk and K. L. Ngai, Molecular dynamics and physical stability of amorphous anti-inflammatory drug: Celecoxib, *J. Phys. Chem. B*, 2010, **114**, 12792.
  - 59 K. Adrjanowicz, D. Zakowiecki, K. Kaminski, L. Hawelek, K. Grzybowska, M. Tarnacka, M. Paluch and K. Cal, Molecular dynamics in supercooled liquid and glassy states of antibiotics: Azithromycin, clarithromycin and roxithromycin studied by dielectric spectroscopy. Advantages given by the amorphous state, *Mol. Pharm.*, 2012, **9**, 1748.
  - 60 J. Knapik, Z. Wojnarowska, K. Grzybowska, L. Hawelek, W. Sawicki, K. Wlodarski, J. Markowski and M. Paluch, Physical stability of the amorphous anticholesterol agent (ezetimibe): The role of molecular mobility, *Mol. Pharm.*, 2014, **11**, 4280.
  - 61 J. Szczurek, M. Rams-Baron, J. Knapik-Kowalczyk, A. Antosik, J. Szafraniec, W. Jamroz, M. Dulski, R. Jachowicz and M. Paluch, Molecular dynamics, recrystallization behavior, and water solubility of the amorphous anticancer agent bicalutamide and its polyvinylpyrrolidone mixtures, *Mol. Pharm.*, 2017, **14**, 1071.
  - 62 A. Mansuri, P. Munzner, T. Feuerbach, A. W. P. Vermeer, W. Hoheisel, R. Bohmer, M. Thommes and C. Gainaru, The relaxation behavior of supercooled and glassy imidacloprid, *J. Chem. Phys.*, 2021, **155**, 174502.
  - 63 G. Adam and J. H. Gibbs, On the temperature dependence of cooperative relaxation properties in glass-forming liquids, *J. Chem. Phys.*, 1965, **43**, 139.
  - 64 I. M. Hodge, Strong and fragile liquids — A brief critique, *J. Non-Cryst. Solids*, 1996, **202**, 164.
  - 65 S. L. Shamblin, X. Tang, L. Chang, B. C. Hancock and M. J. Pikal, Characterization of the time scales of molecular motion in pharmaceutically important glasses, *J. Phys. Chem. B*, 1999, **103**, 4113.
  - 66 B. C. Hancock and S. L. Shamblin, Molecular mobility of amorphous pharmaceuticals determined using differential scanning calorimetry, *Thermochim. Acta*, 2001, **380**, 95.
  - 67 K. Adrjanowicz, K. Grzybowska, K. Kaminski, L. Hawelek, M. Paluch and D. Zakowiecki, Comprehensive studies on physical and chemical stability in liquid and glassy states of telmisartan (TEL): Solubility advantages given by cryomilled and quenched material, *Philos. Mag.*, 2011, **91**, 1926.
  - 68 O. M. H. Salo-Ahen, I. Alanko, R. Bhadane, A. M. J. J. Bonvin, R. V. Honorato, S. Hossain, A. H. Juffer, A. Kabedev, M. Lahtela-Kakkonen, A. S. Larsen, E. Lescrier, P. Marimuthu, M. U. Mirza, G. Mustafa, A. Nunes-Alves, T. Pantsar, A. Saadabadi, K. Singaravelu and M. Vanmeert, Molecular dynamics simulations in drug discovery and pharmaceutical development, *Processes*, 2021, **9**, 71.
  - 69 T. Xiang and B. D. Anderson, Molecular dynamics simulation of amorphous indomethacin-poly (vinylpyrrolidone) glasses: Solubility and hydrogen bonding interactions, *J. Pharm. Sci.*, 2013, **102**, 876.
  - 70 T. Xiang and B. D. Anderson, Molecular dynamics simulation of amorphous hydroxypropylmethylcellulose and its mixtures with felodipine and water, *J. Pharm. Sci.*, 2017, **106**, 803.
  - 71 T. Xiang and B. D. Anderson, Effects of molecular interactions on miscibility and mobility of ibuprofen in amorphous solid dispersions with various polymers, *J. Pharm. Sci.*, 2019, **108**, 178.
  - 72 T. Barnard and G. C. Sosso, Combining machine learning and molecular simulations to predict the stability of amorphous drugs, *J. Chem. Phys.*, 2023, **159**, 014503.
  - 73 L. Larini, A. Ottocian, C. De Michele and D. Leporini, Universal scaling between structural relaxation and vibrational dynamics in glass-forming liquids and polymers, *Nat. Phys.*, 2008, **4**, 42.
  - 74 P. Z. Hanakata, J. F. Douglas and F. W. Starr, Interfacial mobility scale determines the scale of collective motion and relaxation rate in polymer films, *Nat. Commun.*, 2014, **5**, 4163.
  - 75 B. A. P. Betancourt, P. Z. Hanakata, F. W. Starr and J. F. Douglas, Quantitative relations between cooperative motion, emergent elasticity, and free volume in model glass-forming polymer materials, *Proc. Natl. Acad. Sci. U. S. A.*, 2015, **112**, 2966.
  - 76 A. Jaiswal, T. Egami and Y. Zhang, Atomic-scale dynamics of a model glass-forming metallic liquid: Dynamical crossover, dynamical decoupling, and dynamical clustering, *Phys. Rev. B: Condens. Matter Mater. Phys.*, 2015, **91**, 134204.
  - 77 A. Ninarello, L. Berthier and D. Coslovich, Models and algorithms for the next generation of glass transition studies, *Phys. Rev. X*, 2017, **7**, 021039.
  - 78 W. Xu, J. F. Douglas and K. F. Freed, Influence of pressure on glass formation in a simulated polymer melt, *Macromolecules*, 2017, **50**, 2585.
  - 79 J. Hung, T. K. Patra, V. Meenakshisundaram, J. H. Mangalara and D. S. Simmons, Universal localization transition accompanying glass formation: Insights from efficient molecular dynamics simulations of diverse supercooled liquids, *Soft Matter*, 2019, **15**, 1223.
  - 80 L. Berthier and M. D. Ediger, How to “measure” a structural relaxation time that is too long to be measured?, *J. Chem. Phys.*, 2020, **153**, 044501.
  - 81 A. Ghanekarade, A. D. Phan, K. S. Schweizer and D. S. Simmons, Nature of dynamic gradients, glass formation, and collective effects in ultrathin freestanding films, *Proc. Natl. Acad. Sci. U. S. A.*, 2021, **118**, e2104398118.
  - 82 B. Mei, G. S. Sheridan, C. M. Evans and K. S. Schweizer, Elucidation of the physical factors that control activated transport of penetrants in chemically complex glass-forming liquids, *Proc. Natl. Acad. Sci. U. S. A.*, 2022, **119**, e2210094119.



- 83 A. Ghanekarade, A. D. Phan, K. S. Schweizer and D. S. Simmons, Signature of collective elastic glass physics in surface-induced long-range tails in dynamical gradients, *Nat. Phys.*, 2023, **19**, 800.
- 84 S. Mirigian and K. S. Schweizer, Unified theory of activated relaxation in liquids over 14 decades in time, *J. Phys. Chem. Lett.*, 2013, **4**, 3648.
- 85 S. Mirigian and K. S. Schweizer, Elastically cooperative activated barrier hopping theory of relaxation in viscous fluids. I. General formulation and application to hard sphere fluids, *J. Chem. Phys.*, 2014, **140**, 194506.
- 86 S. Mirigian and K. S. Schweizer, Elastically cooperative activated barrier hopping theory of relaxation in viscous fluids. II. Thermal liquids, *J. Chem. Phys.*, 2014, **140**, 194507.
- 87 A. D. Phan, J. Knapik-Kowalczyk, M. Paluch, T. X. Hoang and K. Wakabayashi, Theoretical model for the structural relaxation time in coamorphous drugs, *Mol. Pharm.*, 2019, **16**, 2992.
- 88 A. D. Phan and K. S. Schweizer, Elastically collective nonlinear Langevin equation theory of glass-forming liquids: Transient localization, thermodynamic mapping, and cooperativity, *J. Phys. Chem. B*, 2018, **122**, 8451.
- 89 S. Mirigian and K. S. Schweizer, Dynamical theory of segmental relaxation and emergent elasticity in supercooled polymer melts, *Macromolecules*, 2015, **48**, 1901.
- 90 T. D. Cuong, A. D. Phan, K. Wakabayashi and P. T. Huy, Structural relaxation time and dynamic shear modulus of glassy graphene, *J. Non-Cryst. Solids*, 2020, **538**, 120024.
- 91 A. D. Phan, A. Zaccone, V. D. Lam and K. Wakabayashi, Theory of pressure-induced rejuvenation and strain hardening in metallic glasses, *Phys. Rev. Lett.*, 2021, **126**, 025502.
- 92 T. D. Cuong and A. D. Phan, Effects of cooperative diffusion on rheological and mechanical behavior of bcc Fe: A combined approach using elastically collective nonlinear Langevin equation theory and statistical moment method, *Phys. Rev. B*, 2024, **109**, 054112.
- 93 A. D. Phan, K. Wakabayashi, M. Paluch and V. D. Lam, Effects of cooling rate on structural relaxation in amorphous drugs: Elastically collective nonlinear Langevin equation theory and machine learning study, *RSC Adv.*, 2019, **9**, 40214.
- 94 D. Chen and G. B. McKenna, Deep glassy state dynamic data challenge glass models: Elastic models, *J. Non-Cryst. Solids: X*, 2021, **11–12**, 100068.
- 95 A. D. Phan, Determination of Young's modulus of active pharmaceutical ingredients by relaxation dynamics at elevated pressures, *J. Phys. Chem. B*, 2020, **124**, 10500.
- 96 H. Tanaka, Relationship among glass-forming ability, fragility, and short-range bond ordering of liquids, *J. Non-Cryst. Solids*, 2005, **351**, 678.
- 97 H. Shintani and H. Tanaka, Frustration on the way to crystallization in glass, *Nat. Phys.*, 2006, **2**, 200.
- 98 K. Kawakami, T. Harada, Y. Yoshihashi, E. Yonemochi, K. Terada and H. Moriyama, Correlation between glass-forming ability and fragility of pharmaceutical compounds, *J. Phys. Chem. B*, 2015, **119**, 4873.
- 99 A. D. Phan and K. Wakabayashi, Theory of structural and secondary relaxation in amorphous drugs under compression, *Pharmaceutics*, 2020, **12**, 177.
- 100 T. D. Cuong and A. D. Phan, Compression effects on structural relaxation process of amorphous indomethacin, *Commun. Phys.*, 2021, **31**, 67.
- 101 J. K. Percus and G. J. Yevick, Analysis of classical statistical mechanics by means of collective coordinates, *Phys. Rev.*, 1958, **110**, 1.
- 102 M. S. Wertheim, Exact solution of the Percus-Yevick integral equation for hard spheres, *Phys. Rev. Lett.*, 1963, **10**, 321.
- 103 N. W. Ashcroft and J. Lekner, Structure and resistivity of liquid metals, *Phys. Rev.*, 1966, **145**, 83.
- 104 K. S. Schweizer and E. J. Saltzman, Entropic barriers, activated hopping, and the glass transition in colloidal suspensions, *J. Chem. Phys.*, 2003, **119**, 1181.
- 105 K. S. Schweizer, Derivation of a microscopic theory of barriers and activated hopping transport in glassy liquids and suspensions, *J. Chem. Phys.*, 2005, **123**, 244501.
- 106 E. J. Saltzman and K. S. Schweizer, Activated hopping and dynamical fluctuation effects in hard sphere suspensions and fluids, *J. Chem. Phys.*, 2006, **125**, 044509.
- 107 L. D. Landau and E. M. Lifshitz, *Theory of Elasticity*, Pergamon Press, London, 1975.
- 108 H. A. Kramers, Brownian motion in a field of force and the diffusion model of chemical reactions, *Physica*, 1940, **7**, 284.
- 109 P. Hanggi, P. Talkner and M. Borkovec, Reaction-rate theory: Fifty years after Kramers, *Rev. Mod. Phys.*, 1990, **62**, 251.
- 110 A. D. Phan, N. K. Ngan, D. T. Nga, N. B. Le and C. V. Ha, Tailoring drug mobility by photothermal heating of graphene plasmons, *Phys. Status Solidi RRL*, 2022, **16**, 2100496.
- 111 T. Hecksher and J. C. Dyre, A review of experiments testing the shoving model, *J. Non-Cryst. Solids*, 2015, **407**, 14.
- 112 S. P. Andersson and O. Andersson, Relaxation studies of poly(propylene glycol) under high pressure, *Macromolecules*, 1998, **31**, 2999.
- 113 I. Avramov, A. Grzybowski and M. Paluch, A new approach to description of the pressure dependence of viscosity, *J. Non-Cryst. Solids*, 2009, **355**, 733.
- 114 Z. Wojnarowska, K. Adrjanowicz, P. Włodarczyk, E. Kaminska, K. Kaminski, K. Grzybowska, R. Wrzalik, M. Paluch and K. L. Ngai, Broadband dielectric relaxation study at ambient and elevated pressure of molecular dynamics of pharmaceutical: Indomethacin, *J. Phys. Chem. B*, 2009, **113**, 12536.
- 115 F. D. Murnaghan, The compressibility of media under extreme pressures, *Proc. Natl. Acad. Sci. U. S. A.*, 1944, **30**, 244.
- 116 L. Burakovsky, D. L. Preston and R. R. Silbar, Analysis of dislocation mechanism for melting of elements: Pressure dependence, *J. Appl. Phys.*, 2000, **88**, 6294.





- 117 K. L. Kearns, T. Still, G. Fytas and M. D. Ediger, High-modulus organic glasses prepared by physical vapor deposition, *Adv. Mater.*, 2010, **22**, 39.
- 118 M. Tarnacka, O. Madejczyk, K. Adrjanowicz, J. Pionteck, E. Kaminska, K. Kaminski and M. Paluch, Thermodynamic scaling of molecular dynamics in supercooled liquid state of pharmaceuticals: Itraconazole and ketoconazole, *J. Chem. Phys.*, 2015, **142**, 224507.
- 119 G. Szklarz, K. Adrjanowicz, M. Tarnacka, J. Pionteck and M. Paluch, Confinement-induced changes in the glassy dynamics and crystallization behavior of supercooled fenofibrate, *J. Phys. Chem. C*, 2018, **122**, 1384.
- 120 P. I. Dorogokupets, A. M. Dymshits, K. D. Litasov and T. S. Sokolova, Thermodynamics and equations of state of iron to 350 GPa and 6000 K, *Sci. Rep.*, 2017, **7**, 41863.
- 121 O. L. Anderson, *Equations of State of Solids for Geophysics and Ceramic Science*, Oxford University Press, New York, 1995.
- 122 A. K. Pandey and B. K. Pandey, Rahul, Theoretical prediction of Grüneisen parameter for bulk metallic glasses, *J. Alloys Compd.*, 2011, **509**, 4191.
- 123 K. S. Schweizer and G. Yatsenko, Collisions, caging, thermodynamics, and jamming in the barrier hopping theory of glassy hard sphere fluids, *J. Chem. Phys.*, 2007, **127**, 164505.
- 124 R. Kubo, Statistical-mechanical theory of irreversible processes. I. General theory and simple applications to magnetic and conduction problems, *J. Phys. Soc. Jpn.*, 1957, **12**, 570.
- 125 B. Shi, S. Yang, S. Liu and P. Jin, Lindemann-like rule between average thermal expansion coefficient and glass transition temperature for metallic glasses, *J. Non-Cryst. Solids*, 2019, **503**, 194.
- 126 M. Guinan and D. Steinberg, A simple approach to extrapolating measured polycrystalline shear moduli to very high pressure, *J. Phys. Chem. Solids*, 1975, **36**, 829.
- 127 L. Burakovsky and D. L. Preston, Generalized Guinan-Steinberg formula for the shear modulus at all pressures, *Phys. Rev. B: Condens. Matter Mater. Phys.*, 2005, **71**, 184118.
- 128 V. Mazel, V. Busignies, H. Diarra and P. Tchoreloff, On the links between elastic constants and effective elastic behavior of pharmaceutical compacts: Importance of Poisson's ratio and use of bulk modulus, *J. Pharm. Sci.*, 2013, **102**, 4009.
- 129 G. Arfken, *Mathematical Methods for Physicists*, Academic Press, Orlando, 1985.
- 130 K. Adrjanowicz, A. Grzybowski, K. Kaminski and M. Paluch, Temperature and volume effect on the molecular dynamics of supercooled ibuprofen at ambient and elevated pressure, *Mol. Pharm.*, 2011, **8**, 1975.
- 131 K. Adrjanowicz, K. Kaminski, M. Paluch and K. Niss, Crystallization behavior and relaxation dynamics of supercooled S-ketoprofen and the racemic mixture along an isochrone, *Cryst. Growth Des.*, 2015, **15**, 3257.
- 132 E. Kaminska, A. Minecka, M. Tarnacka, K. Kaminski and M. Paluch, Breakdown of the isochronal structural ( $\alpha$ ) and secondary (JG  $\beta$ ) exact superpositioning in probucol—A low molecular weight pharmaceutical, *J. Mol. Liq.*, 2020, **299**, 112169.
- 133 D. Heczko, K. Jurkiewicz, J. Grelska, K. Kaminski, M. Paluch and E. Kaminska, Influence of high pressure on the local order and dynamical properties of the selected azole antifungals, *J. Phys. Chem. B*, 2020, **124**, 11949.
- 134 P. Jesionek, D. Heczko, B. Hachuła, K. Kaminski and E. Kaminska, High-pressure studies in the supercooled and glassy state of the strongly associated active pharmaceutical ingredient—Ticagrelor, *Sci. Rep.*, 2023, **13**, 8890.
- 135 G. Szklarz, K. Adrjanowicz, M. Dulski, J. Knapik and M. Paluch, Dielectric relaxation study at ambient and elevated pressure of the modeled lipophilic drug fenofibrate, *J. Phys. Chem. B*, 2016, **120**, 11298.
- 136 M. Tarnacka, K. Adrjanowicz, E. Kaminska, K. Kaminski, K. Grzybowska, K. Kolodziejczyk, P. Włodarczyk, L. Hawelek, G. Garbacz, A. Kocot and M. Paluch, Molecular dynamics of itraconazole at ambient and high pressure, *Phys. Chem. Chem. Phys.*, 2013, **15**, 20742.
- 137 Z. Wojnarowska, K. Adrjanowicz, K. Kaminski, L. Hawelek and M. Paluch, Effect of pressure on tautomers' equilibrium in supercooled glibenclamide drug: Analysis of fragility behavior, *J. Phys. Chem. B*, 2010, **114**, 14815.
- 138 K. Adrjanowicz, Z. Wojnarowska, M. Paluch and J. Pionteck, Thermodynamic scaling of molecular dynamics in supercooled ibuprofen, *J. Phys. Chem. B*, 2011, **115**, 4559.
- 139 Z. Wojnarowska, K. Grzybowska, K. Adrjanowicz, K. Kaminski, M. Paluch, L. Hawelek, R. Wrzałik, M. Dulski, W. Sawicki, J. Mazgalski, A. Tukalska and T. Bieg, Study of the amorphous glibenclamide drug: Analysis of the molecular dynamics of quenched and cryomilled material, *Mol. Pharm.*, 2010, **7**, 1692.
- 140 Z. Wojnarowska, P. Włodarczyk, K. Kaminski, K. Grzybowska, L. Hawelek and M. Paluch, On the kinetics of tautomerism in drugs: New application of broadband dielectric spectroscopy, *J. Chem. Phys.*, 2010, **133**, 094507.
- 141 Z. Wojnarowska, M. Paluch and J. Pionteck, The tautomerization phenomenon of glibenclamide drug monitored by means of volumetric measurements, *J. Chem. Phys.*, 2011, **135**, 214506.
- 142 C. A. Angell, Relaxation in liquids, polymers and plastic crystals — Strong/fragile patterns and problems, *J. Non-Cryst. Solids*, 1991, **131**, 13.
- 143 C. M. Roland, S. Hensel-Bielowka, M. Paluch and R. Casalini, Supercooled dynamics of glass-forming liquids and polymers under hydrostatic pressure, *Rep. Prog. Phys.*, 2005, **68**, 1405.
- 144 R. Casalini and C. M. Roland, Scaling of the supercooled dynamics and its relation to the pressure dependences of the dynamic crossover and the fragility of glass formers, *Phys. Rev. B: Condens. Matter Mater. Phys.*, 2005, **71**, 014210.
- 145 M. Paluch, E. Masiewicz, A. Grzybowski, S. Pawlus, J. Pionteck and Z. Wojnarowska, General rules prospected for the liquid fragility in various material groups and



- different thermodynamic conditions, *J. Chem. Phys.*, 2014, **141**, 134507.
- 146 E. Masiewicz, A. Grzybowski, A. P. Sokolov and M. Paluch, Temperature–volume entropic model for viscosities and structural relaxation times of glass formers, *J. Phys. Chem. Lett.*, 2012, **3**, 2643.
  - 147 P. Lunkenheimer, A. Loidl, B. Riechers, A. Zaccone and K. Samwer, Thermal expansion and the glass transition, *Nat. Phys.*, 2023, **19**, 694.
  - 148 D. Zhou, G. G. Z. Zhang, D. Law, D. J. W. Grant and E. A. Schmitt, Physical stability of amorphous pharmaceuticals: Importance of configurational thermodynamic quantities and molecular mobility, *J. Pharm. Sci.*, 2002, **91**, 1863.
  - 149 J. A. Baird, B. V. Eerdenbrugh and L. S. Taylor, A classification system to assess the crystallization tendency of organic molecules from undercooled melts, *J. Pharm. Sci.*, 2010, **99**, 3787.
  - 150 U. Sailaja, M. S. Thayyil, N. S. K. Kumar and G. Govindaraj, Molecular dynamics of amorphous pharmaceutical fenofibrate studied by broadband dielectric spectroscopy, *J. Pharm. Anal.*, 2016, **6**, 165.
  - 151 W. Tu, X. Li, Z. Chen, Y. D. Liu, M. Labardi, S. Capaccioli, M. Paluch and L. M. Wang, Glass formability in medium-sized molecular systems/pharmaceuticals. I. Thermodynamics vs. kinetics, *J. Chem. Phys.*, 2016, **144**, 174502.
  - 152 R. Casalini, M. Paluch and C. M. Roland, Influence of molecular structure on the dynamics of supercooled van der Waals liquids, *Phys. Rev. E*, 2003, **67**, 031505.
  - 153 K. Grzybowska, M. Paluch, A. Grzybowski, S. Pawlus, S. Ancherbak, D. Prevosto and S. Capaccioli, Dynamic crossover of water relaxation in aqueous mixtures: Effect of pressure, *J. Phys. Chem. Lett.*, 2010, **1**, 1170.
  - 154 D. Chandler and H. C. Andersen, Optimized cluster expansions for classical fluids. II. Theory of molecular liquids, *J. Chem. Phys.*, 1972, **57**, 1930.
  - 155 K. S. Schweizer and J. G. Curro, Integral equation theories of the structure, thermodynamics, and phase transitions of polymer fluids, *Adv. Chem. Phys.*, 1997, **98**, 1.
  - 156 J. P. Hansen and I. R. McDonald, *Theory of Simple Liquids*, Academic Press, London, 2006.
  - 157 Z. E. Dell and K. S. Schweizer, Microscopic theory for the role of attractive forces in the dynamics of supercooled liquids, *Phys. Rev. Lett.*, 2015, **115**, 205702.
  - 158 A. Ghosh and K. S. Schweizer, Microscopic theory of the influence of strong attractive forces on the activated dynamics of dense glass and gel forming fluids, *J. Chem. Phys.*, 2019, **151**, 244502.
  - 159 A. Ghosh and K. S. Schweizer, Microscopic theory of onset of decaging and bond-breaking activated dynamics in ultradense fluids with strong short-range attractions, *Phys. Rev. E*, 2020, **101**, 060601(R).
  - 160 A. Minecka, B. Hachula, K. Kaminski, M. Paluch and E. Kaminska, How does pressure affect the molecular dynamics, intramolecular interactions, and the relationship between structural ( $\alpha$ ) and secondary ( $\beta$ -JG) relaxation above and below the glass transition temperature in binary mixtures of H-bonded API – Probutol and acetylated saccharides?, *Eur. J. Pharm. Sci.*, 2021, **164**, 105894.
  - 161 A. Minecka, M. Tarnacka, K. Jurkiewicz, B. Hachula, K. Kaminski, M. Paluch and E. Kaminska, Influence of the internal structure and intermolecular interactions on the correlation between structural ( $\alpha$ ) and secondary ( $\beta$ -JG) relaxation below the glass transition temperature in neat probucol and its binary mixtures with modified saccharides, *J. Phys. Chem. B*, 2020, **124**, 4821.
  - 162 P. D. Ispanovity, I. Groma, G. Gyorgyi, P. Szabo and W. Hoffelner, Criticality of relaxation in dislocation systems, *Phys. Rev. Lett.*, 2011, **107**, 085506.
  - 163 J. Rottler, S. S. Schoenholz and A. J. Liu, Predicting plasticity with soft vibrational modes: From dislocations to glasses, *Phys. Rev. E*, 2014, **89**, 042304.
  - 164 X. Wang, F. Maresca and P. Cao, The hierarchical energy landscape of screw dislocation motion in refractory high-entropy alloys, *Acta Mater.*, 2022, **234**, 118022.
  - 165 B. Bako, I. Groma, G. Gyorgyi and G. T. Zimanyi, Dislocation glasses: Aging during relaxation and coarsening, *Phys. Rev. Lett.*, 2007, **98**, 075701.
  - 166 S. J. Gerbode, U. Agarwal, D. C. Ong, C. M. Liddell, F. Escobedo and I. Cohen, Glassy dislocation dynamics in 2D colloidal dimer crystals, *Phys. Rev. Lett.*, 2010, **105**, 078301.
  - 167 P. D. Ispanovity, L. Laurson, M. Zaiser, I. Groma, S. Zapperi and M. J. Alava, Avalanches in 2D dislocation systems: Plastic yielding Is not depinning, *Phys. Rev. Lett.*, 2014, **112**, 235501.
  - 168 A. Lehtinen, G. Costantini, M. J. Alava, S. Zapperi and L. Laurson, Glassy features of crystal plasticity, *Phys. Rev. B*, 2016, **94**, 064101.
  - 169 M. Ovaska, A. Lehtinen, M. J. Alava, L. Laurson and S. Zapperi, Excitation spectra in crystal plasticity, *Phys. Rev. Lett.*, 2017, **119**, 265501.
  - 170 L. Burakovsky, D. L. Preston and R. R. Silbar, Melting as a dislocation-mediated phase transition, *Phys. Rev. B: Condens. Matter Mater. Phys.*, 2000, **61**, 15011.
  - 171 L. Gomez, A. Dobry, Ch. Geuting, H. T. Diep and L. Burakovsky, Dislocation lines as the precursor of the melting of crystalline solids observed in Monte Carlo simulations, *Phys. Rev. Lett.*, 2003, **90**, 095701.
  - 172 L. Burakovsky, C. W. Greeff and D. L. Preston, Analytic model of the shear modulus at all temperatures and densities, *Phys. Rev. B: Condens. Matter Mater. Phys.*, 2003, **67**, 094107.
  - 173 W. Kauzmann, The nature of the glassy state and the behavior of liquids at low temperatures, *Chem. Rev.*, 1948, **43**, 219.
  - 174 R. Clausius, Über die bewegende kraft der wärme und die gesetze, welche sich daraus für die wärmelehre selbst ableiten lassen, *Ann. Phys.*, 1850, **155**, 368.
  - 175 M. C. Clapeyron, Mémoire sur la puissance motrice de la chaleur, *J. Ec. Polytech.*, 1834, **23**, 153.



- 176 C. A. Angell, Formation of glasses from liquids and biopolymers, *Science*, 1995, **267**, 1924.
- 177 M. Kazmierczak, E. Patyk-Kazmierczak and A. Katrusiak, Compression and thermal expansion in organic and metal-organic crystals: The pressure-temperature correspondence rule, *Cryst. Growth Des.*, 2021, **21**, 2196.
- 178 O. N. Senkov and D. B. Miracle, Correlation between thermodynamic and kinetic properties of glass-forming liquids, *Mater. Res. Soc. Symp. Proc.*, 2008, **1048**, 10.
- 179 C. R. Groom, I. J. Bruno, M. P. Lightfoot and S. C. Ward, The Cambridge Structural Database, *Acta Crystallogr., Sect. B: Struct. Sci., Cryst. Eng. Mater.*, 2016, **72**, 171.
- 180 P. Sanphui, B. Sarma and A. Nangia, Phase transformation in conformational polymorphs of nimesulide, *J. Pharm. Sci.*, 2011, **100**, 2287.
- 181 E. J. Chan and D. J. Goossens, Study of the single-crystal X-ray diffuse scattering in paracetamol polymorphs, *Acta Crystallogr., Sect. B: Struct. Sci.*, 2012, **68**, 80.
- 182 J. J. Gerber, M. R. Caira and A. P. Lotter, Structures of two conformational polymorphs of the cholesterol-lowering drug probucol, *J. Crystallogr. Spectrosc. Res.*, 1993, **23**, 863.
- 183 L. D. Prado, H. V. A. Rocha, J. A. L. C. Resende, G. B. Ferreira and A. M. R. de Figueiredo Teixeira, An insight into carvedilol solid forms: Effect of supramolecular interactions on the dissolution profiles, *CrystEngComm*, 2014, **16**, 3168.
- 184 D. Csicsak, E. Borbas, S. Kadar, P. Tozser, P. Bagi, H. Pataki, B. Sinko, K. Takacs-Novak and G. Volgyi, Towards more accurate solubility measurements with real time monitoring: a carvedilol case study, *New J. Chem.*, 2021, **45**, 11618.
- 185 K. Koperwas, A. Grzybowski, K. Grzybowska, Z. Wojnarowska and M. Paluch, Effects of dynamic heterogeneity and density scaling of molecular dynamics on the relationship among thermodynamic coefficients at the glass transition, *J. Chem. Phys.*, 2015, **143**, 024502.
- 186 K. Chmiel, J. Knapik-Kowalczyk, E. Kaminska, L. Tajber and M. Paluch, High-pressure dielectric studies—A way to experimentally determine the solubility of a drug in the polymer matrix at low temperatures, *Mol. Pharm.*, 2021, **18**, 3050.
- 187 T. A. Lima, L. F. O. Faria, V. H. Paschoal and M. C. C. Ribeiro, Communication: Glass transition and melting lines of an ionic liquid, *J. Chem. Phys.*, 2018, **148**, 171101.
- 188 J. Ledru, C. T. Imrie, C. R. Pulham, R. Ceolin and J. M. Hutchinson, High pressure differential scanning calorimetry investigations on the pressure dependence of the melting of paracetamol polymorphs I and II, *J. Pharm. Sci.*, 2007, **96**, 2784.
- 189 G. B. McKenna and S. L. Simon, 50th anniversary perspective: Challenges in the dynamics and kinetics of glass-forming polymers, *Macromolecules*, 2017, **50**, 6333.
- 190 J. Knapik, Z. Wojnarowska, K. Grzybowska, L. Tajber, H. Mesallati, K. J. Paluch and M. Paluch, Molecular dynamics and physical stability of amorphous nimesulide drug and its binary drug-polymer systems, *Mol. Pharm.*, 2016, **13**, 1937.
- 191 A. A. Ravikumar, P. K. Kulkarni, R. A. M. Osmani, U. Hani, M. Ghazwani, A. A. Fatease, A. H. Alamri and D. V. Gowda, Carvedilol precipitation inhibition by the incorporation of polymeric precipitation inhibitors using a stable amorphous solid dispersion approach: Formulation, characterization, and *in vitro in vivo* evaluation, *Polymers*, 2022, **14**, 4977.
- 192 J. Knapik-Kowalczyk, Z. Wojnarowska, M. Rams-Baron, K. Jurkiewicz, J. Cielecka-Piontek, K. L. Ngai and M. Paluch, Atorvastatin as a promising crystallization inhibitor of amorphous probucol: Dielectric studies at ambient and elevated pressure, *Mol. Pharm.*, 2017, **14**, 2670.
- 193 G. P. Johari, S. Kim and R. M. Shanker, Dielectric studies of molecular motions in amorphous solid and ultraviscous acetaminophen, *J. Pharm. Sci.*, 2005, **94**, 2207.
- 194 K. Yamaguchi, R. Mizoguchi, K. Kawakami and T. Miyazaki, Influence of the crystallization tendencies of pharmaceutical glasses on the applicability of the Adam-Gibbs-Vogel and Vogel-Tammann-Fulcher equations in the prediction of their long-term physical stability, *Int. J. Pharm.*, 2022, **626**, 122158.
- 195 A. Minecka, B. Hachuła, K. Jurkiewicz, K. Kaminski, M. Paluch and E. Kaminska, High pressure aging studies on the low-molecular weight glass-forming pharmaceutical – Probucol, *J. Mol. Liq.*, 2021, **321**, 114626.
- 196 P. Lunkenheimer and A. Loidl, Glassy dynamics: From millihertz to terahertz, in *The Scaling of Relaxation Processes*, ed. F. Kremer and A. Loidl, Springer, Cham, 2018, p. 23.
- 197 K. Chen and K. S. Schweizer, Molecular theory of physical aging in polymer glasses, *Phys. Rev. Lett.*, 2007, **98**, 167802.
- 198 F. Arceri, F. P. Landes, L. Berthier, and G. Biroli, Glasses and aging, a statistical mechanics perspective on, in *Statistical and Nonlinear Physics*, ed. B. Chakraborty, Springer, New York, 2022, p. 229.
- 199 B. Riechers, L. A. Roed, S. Mehri, T. S. Ingebrigtsen, T. Hecksher, J. C. Dyre and K. Niss, Predicting nonlinear physical aging of glasses from equilibrium relaxation via the material time, *Sci. Adv.*, 2022, **8**, eabl9809.
- 200 T. Bohmer, J. P. Gabriel, L. Costigliola, J. N. Kociok, T. Hecksher, J. C. Dyre and T. Blochowicz, Time reversibility during the ageing of materials, *Nat. Phys.*, 2024, **20**, 637.

